

Mfront user day 2023

Microstructure-based modelling of snow viscoplasticity using FFT-based simulations and MFront to model crystal plasticity

Louis Védrine^{1 2}, Pascal Hagenmuller¹, Maurine Montagnat^{1 3},
Lionel Gélébart⁴, Antoine Bernard^{1 3}, Henning Löwe⁵

¹ Univ. Grenoble Alpes, Univ. de Toulouse, Météo-France, CNRS, CNRM, Centre d'Études de la Neige, Grenoble, France

² Univ. Paris-Saclay, ENS Paris-Saclay, DER Génie Civil et Environnement, Gif-sur-Yvette, France

³ Univ. Grenoble Alpes, Grenoble-INP, CNRS, IRD, Institut des Géosciences de l'Environnement, Grenoble, France

⁴ Univ. Paris-Saclay, CEA, Service de Recherches Métallurgiques Appliquées, 91191, Gif-sur-Yvette, France

⁵ WSL Institute for Snow and Avalanche Research SLF, Davos Dorf, Switzerland

Context: what is snow settlement?



T= 0 h

*Winter storm in Virginia (USA) between January 22 and 24, 2016,
adapted from WorseThanChiggers*

Context: what is snow settlement?



T= 16 h

*Winter storm in Virginia (USA) between January 22 and 24, 2016,
adapted from WorseThanChiggers*

Context: what is snow settlement?



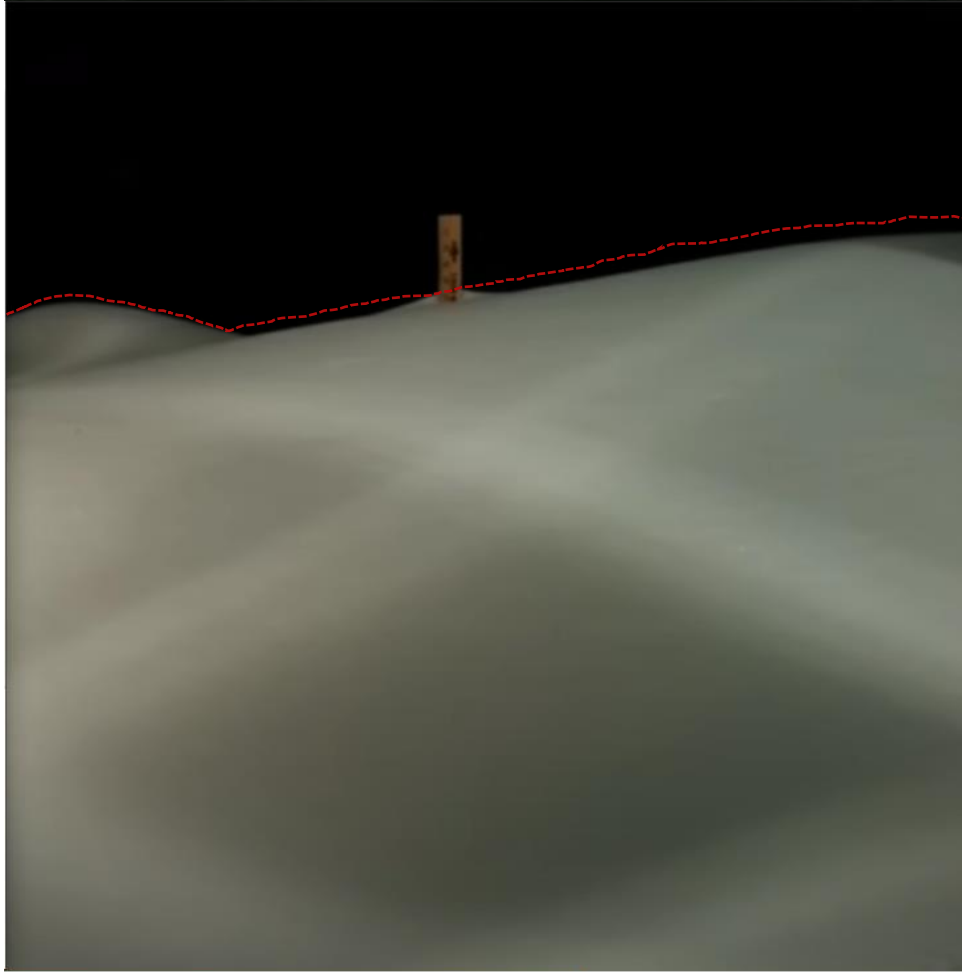
The snowflake that falls out of the sky doesn't stay that way for long...

T= 35 h



*Winter storm in Virginia (USA) between January 22 and 24, 2016,
adapted from WorseThanChiggers*

Context: what is snow settlement?



The snowflake that falls out of the sky doesn't stay that way for long

The snowflakes change their form and become more rounded

Settlement is the **slow** deformation of the snow as it densifies and sags under the influence of **gravity**

T= 38 h

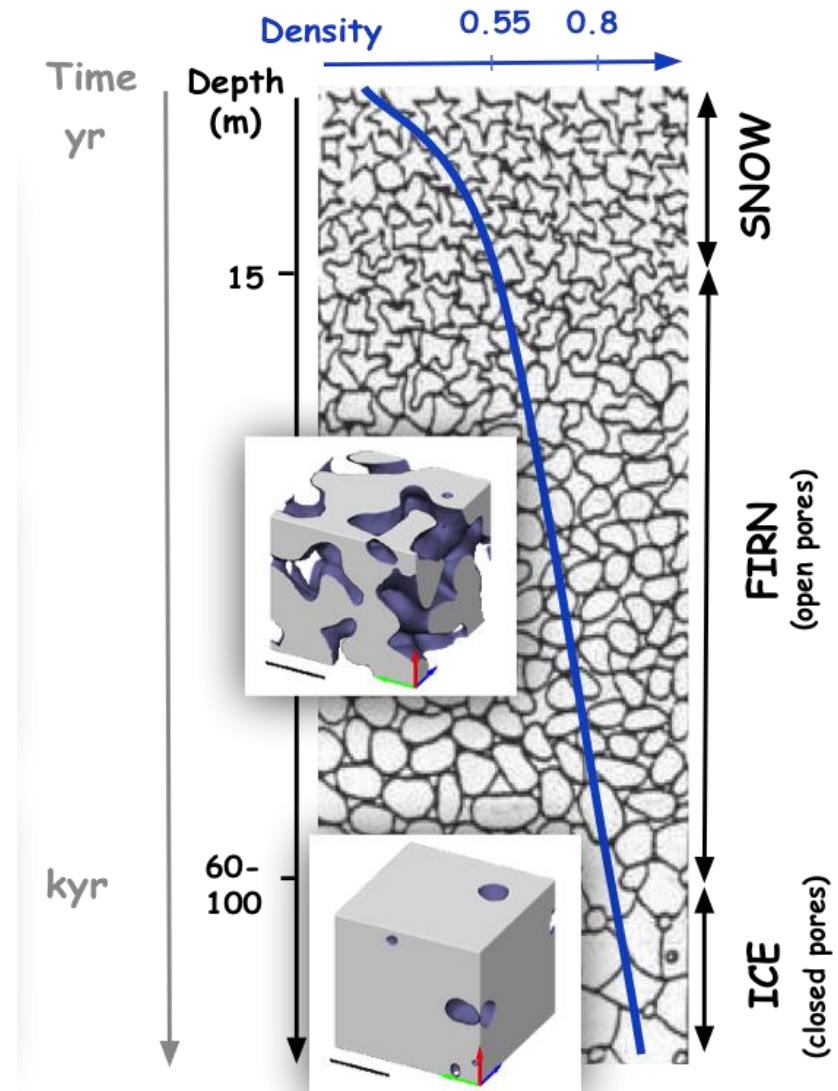
Winter storm in Virginia (USA) between January 22 and 24, 2016,
adapted from WorseThanChiggers

Context: applications

- Snowpack modelling, Paleoclimatology ...



Snowboarder Mathieu Schaer. Credit: Ruedi Flueck



Schematic view of the snow-firn ice Continuum (Dumont et al., 2020)

Context: snow microstructure

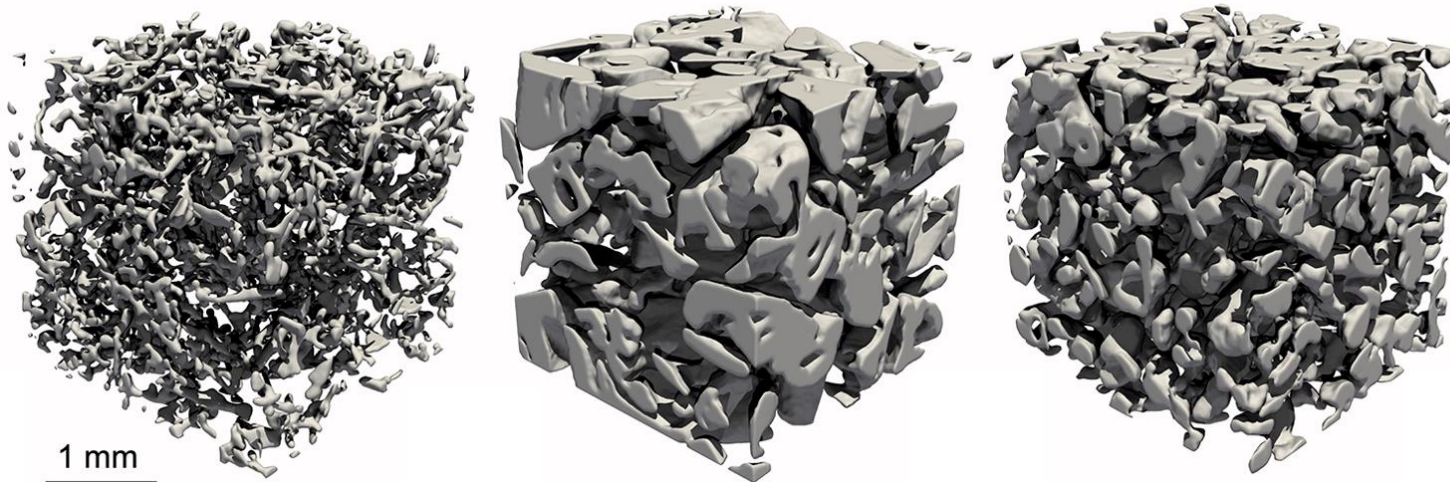
Snow = mixture of ice crystals sintered together, air and sometimes liquid water and impurities.

Material close to the melting temperature

Porosity → 95% fresh snow / 10% for dense firn

Large number of snow type → difficult to characterize

Snow settlement is mainly driven by the creep of the **ice matrix** undergoing **viscoplastic deformations**



Three-dimensional view of the microstructure of some representative snow samples. Measured with X-ray microtomography by Lin et al., (2022).



Cup-shaped crystals in the snowpack (SLF).

Scientific questions:

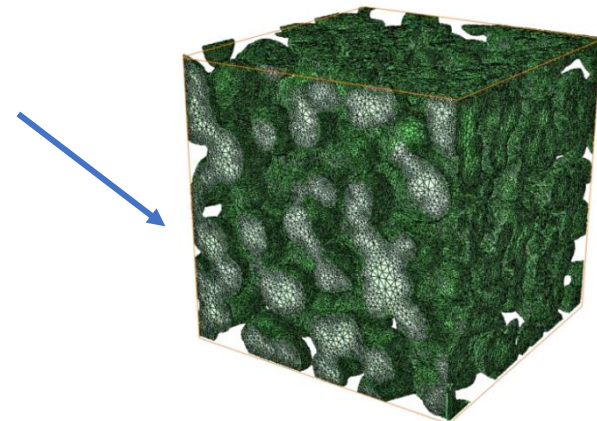
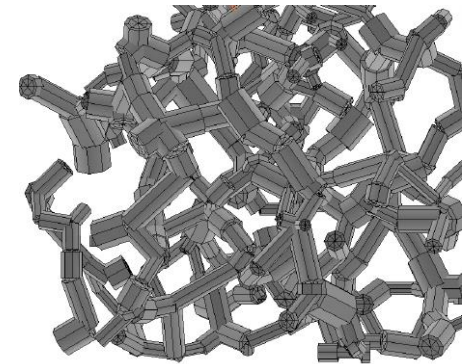
- How does the viscoplastic behaviour of ice scales to the snow mechanical behaviour?

Key bibliography:

Investigation through microstructure-based simulations :

snow = 3D microstructure + ice mechanical properties

- *Theile et al., (2011)*: highly simplified snow microstructure + advanced modelling of ice mechanics
- *Wautier et al., (2017)*: faithful microstructure + rough ice mechanics



Scientific questions:

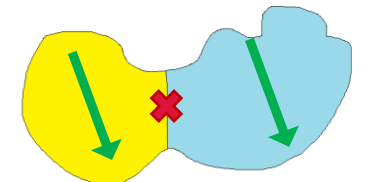
- How does the viscoplastic behaviour of ice scale to the snow mechanical behaviour?

Our work:

- Microstructure-based simulation: faithful microstructure + advanced ice mechanics, made possible via a suitable solver: AMITEX
- Direct evaluation based on previous creep experiments captured by tomography.

Contours of the study:

- Study of dry snow only, under isothermal conditions without metamorphism ;
- Account only intra-crystalline deformation (inter-crystalline sliding is overlooked).



Methodology: experimental setup

As our model **cannot reproduce the evolution of the microstructure**, we use the **set of experimentally obtained microstructures** to decompose the test into a set of instantaneous creep experiments.

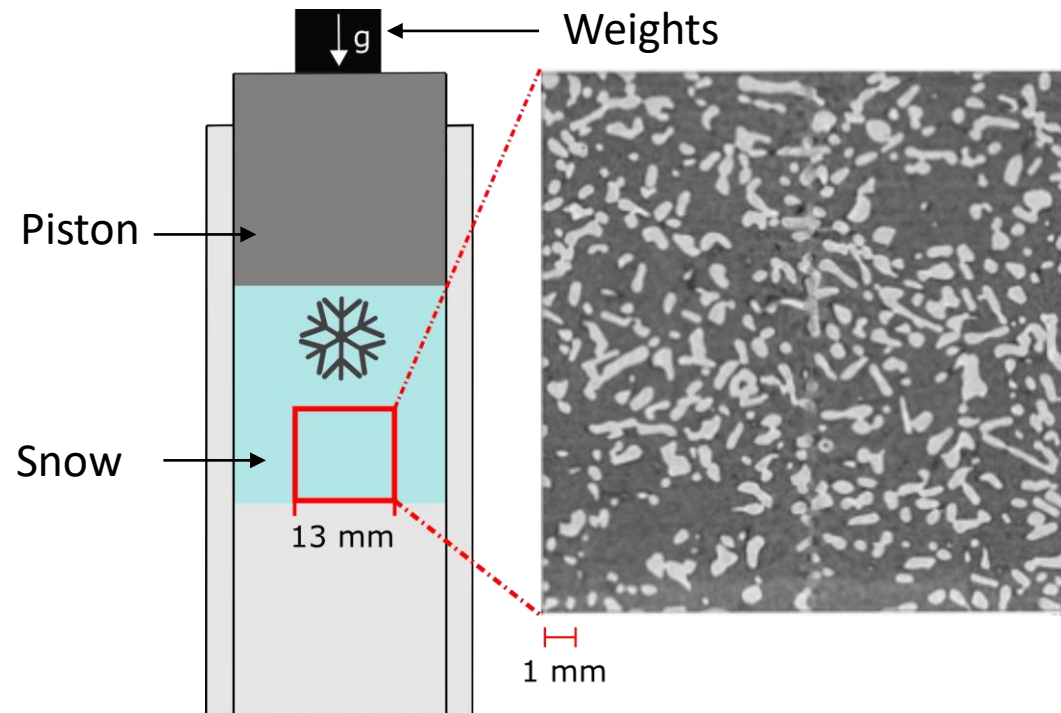
We use two mechanical tests performed by (*Bernard et al., 2022*):

I) Load-controlled test:

- $\sigma_{\text{imp}} = 2.1 \text{ kPa}$, $T_{\text{snow}} = -8 \pm 0.5 \text{ }^{\circ}\text{C}$
- Deformation determined based on density measurement (X-Ray tomography)



Tomograph (Hagenmuller)



Experimental setup (Bernard et al., 2022)

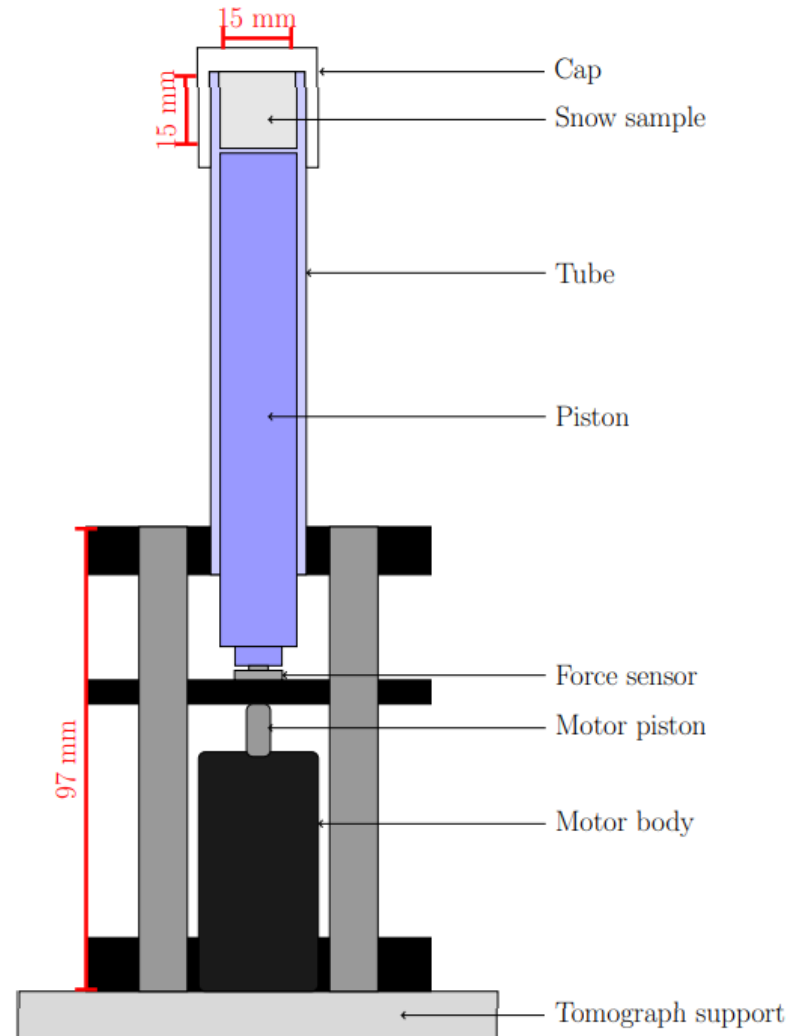
Methodology: experimental setup

As our model **cannot reproduce the evolution of the microstructure**, we use the **set of experimentally obtained microstructures** to decompose the test into a set of instantaneous creep experiments.

We use two mechanical tests performed by (*Bernard et al., 2022-2023*):

II) Strain-rate-controlled compression test:

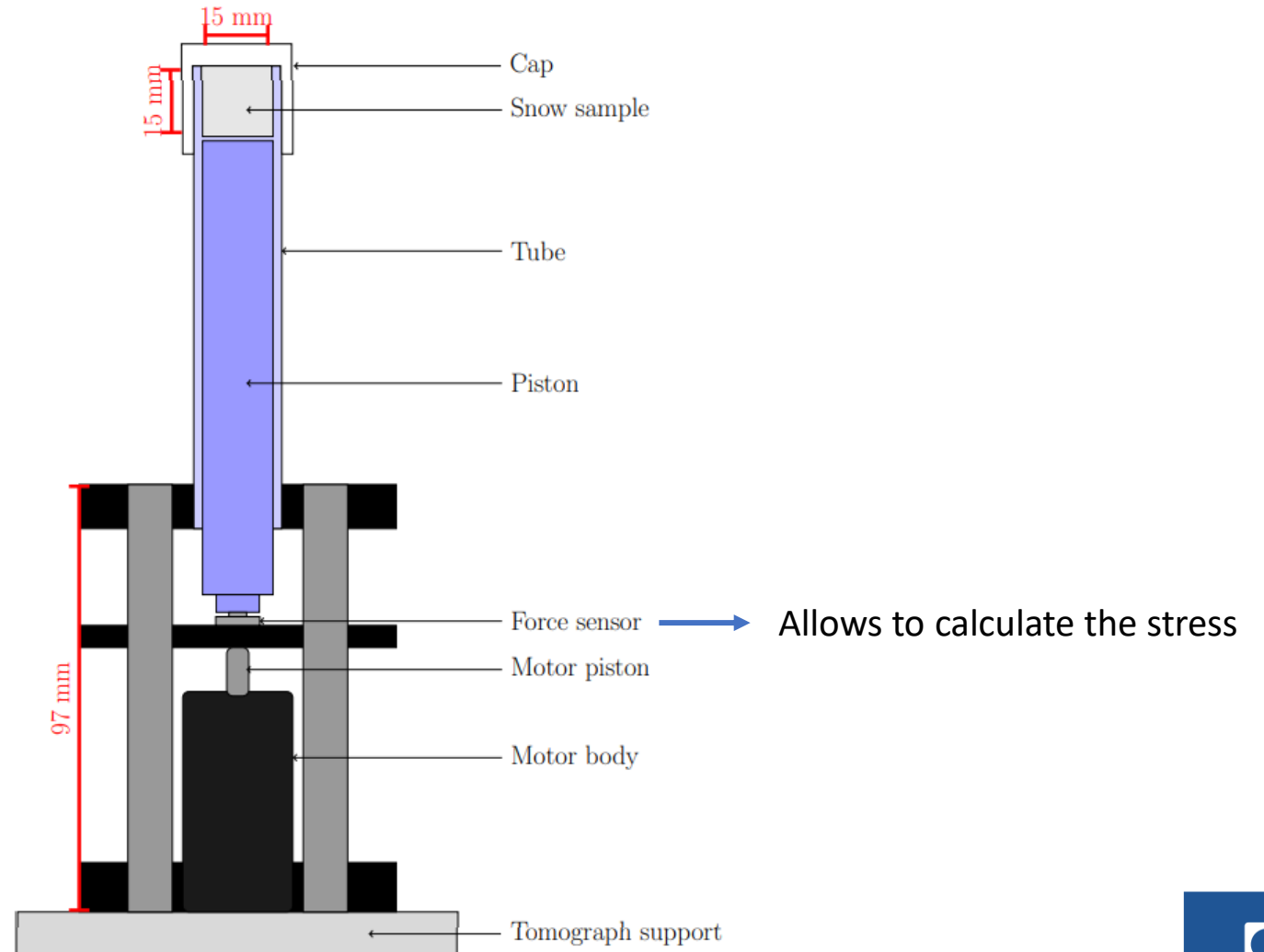
- $\dot{\epsilon}_{\text{imp}} = 1.8 \times 10^{-6} \text{ s}^{-1}$,
- $T_{\text{snow}} = -18 \pm 0.5 \text{ }^{\circ}\text{C}$



Experimental setup (*Bernard et al., 2023*)

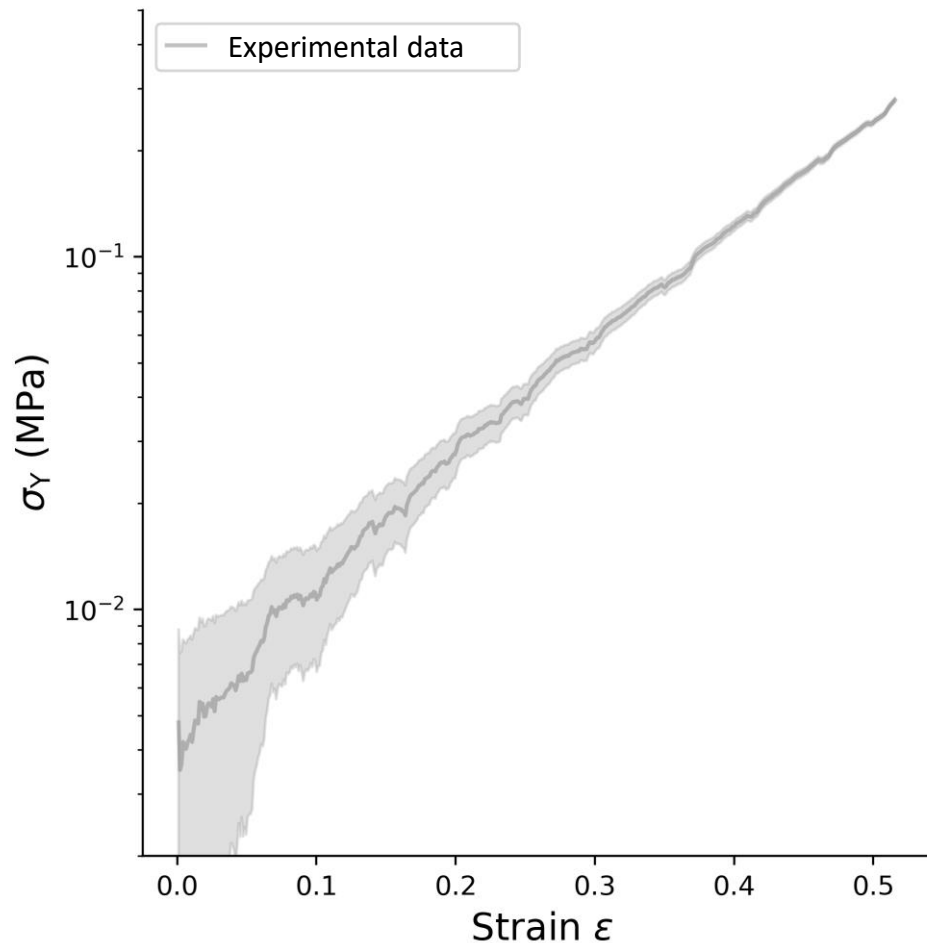
Methodology: experimental setup

Strain-rate-controlled compression test

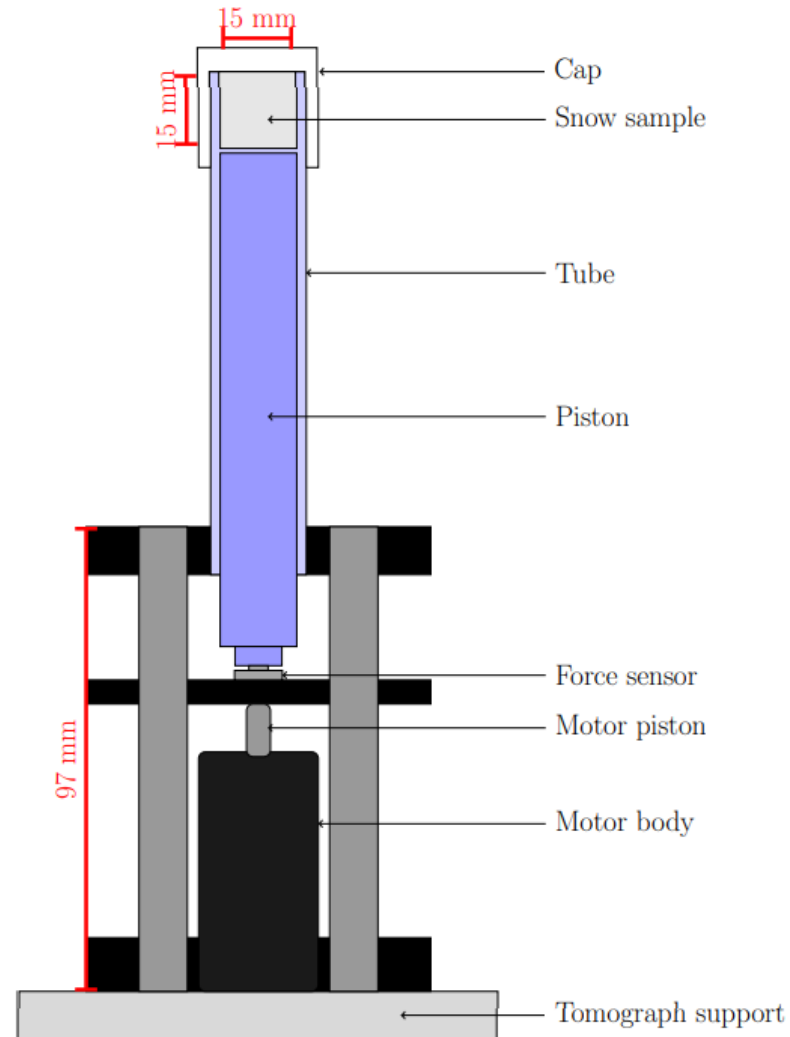


Experimental setup (Bernard et al., 2023)

Methodology: experimental setup

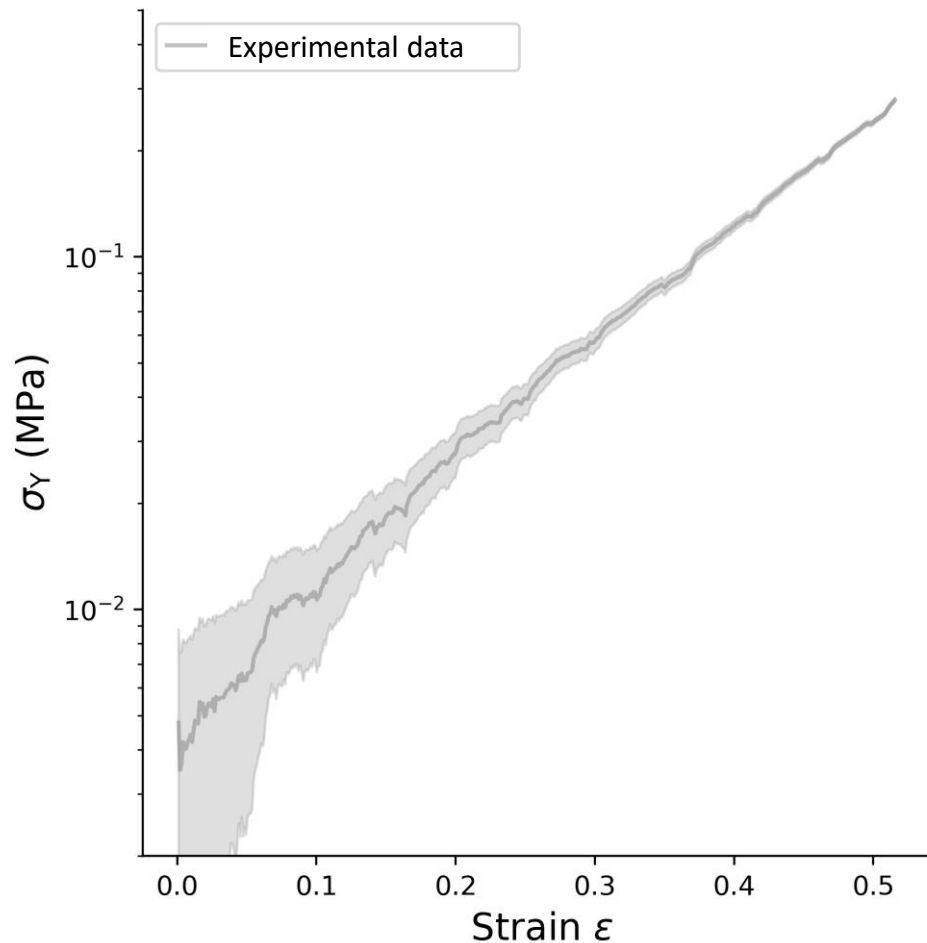


Strain-rate-controlled compression test

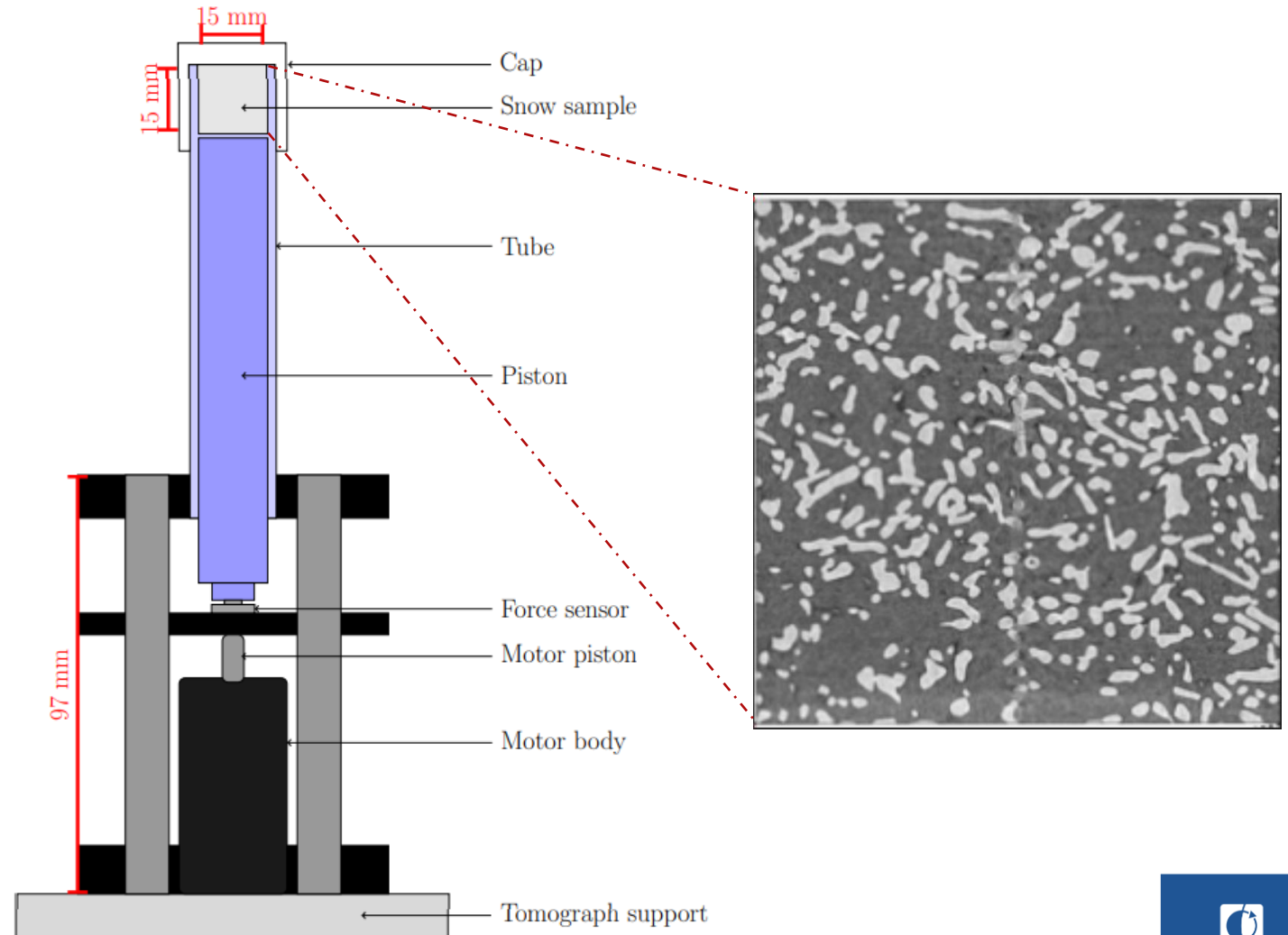


Experimental setup (Bernard et al., 2023)

Methodology: experimental setup

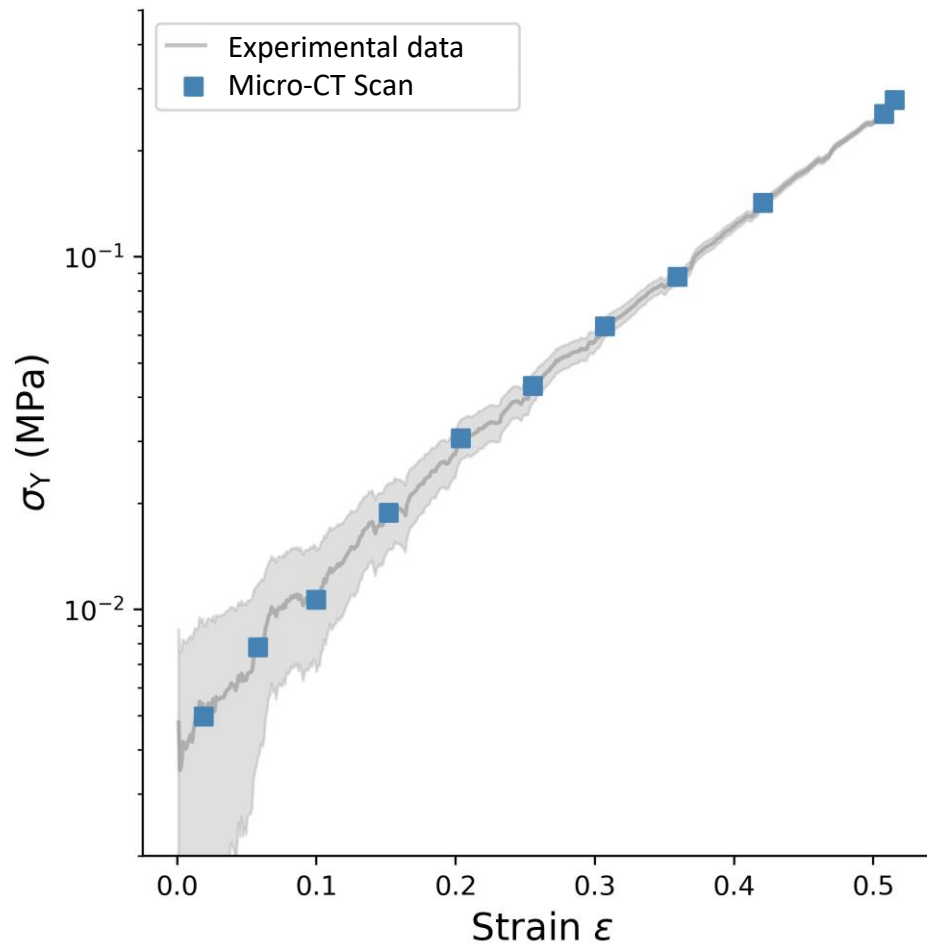


Strain-rate-controlled compression test

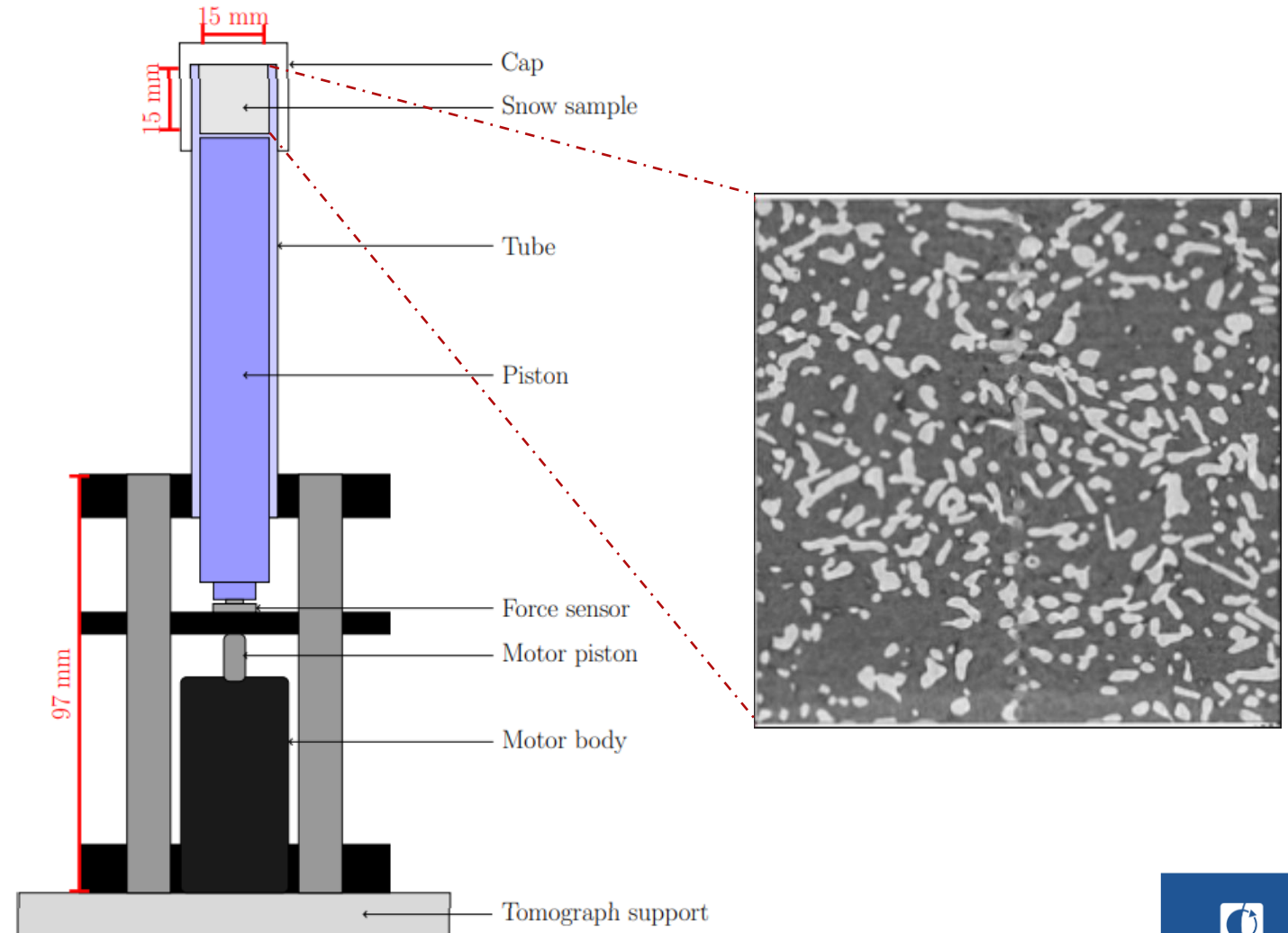


Experimental setup (Bernard et al., 2023)

Methodology: experimental setup

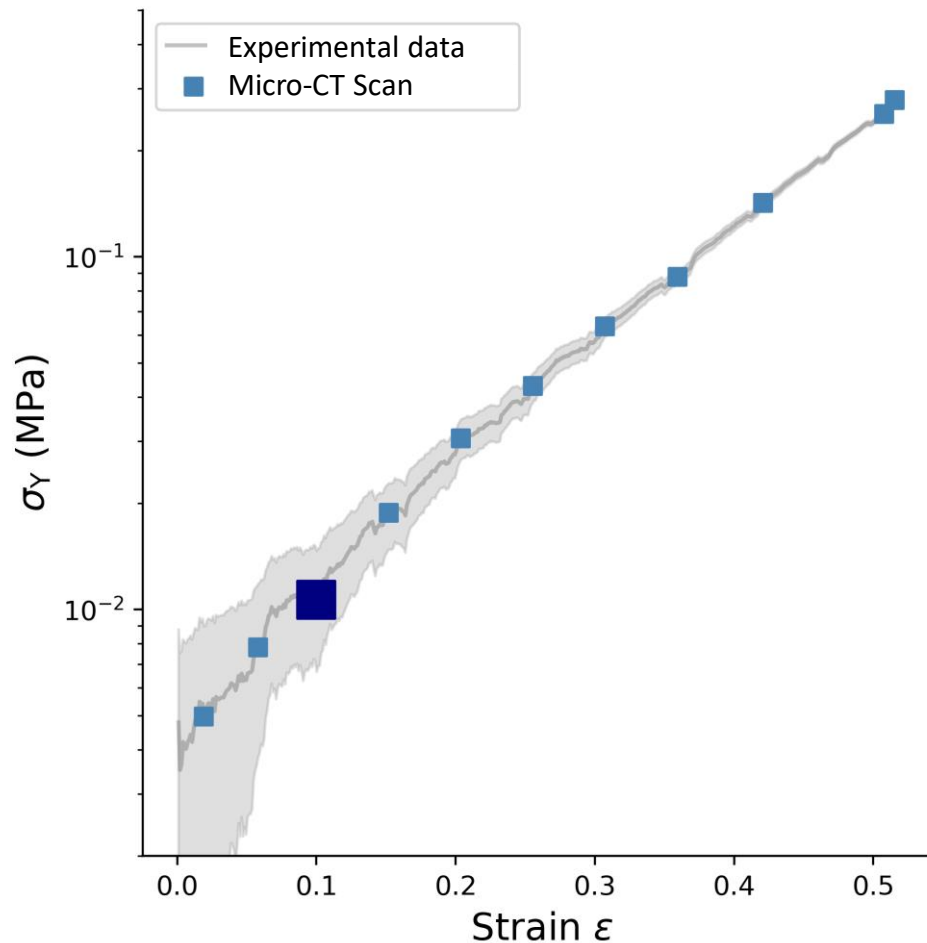


Strain-rate-controlled compression test

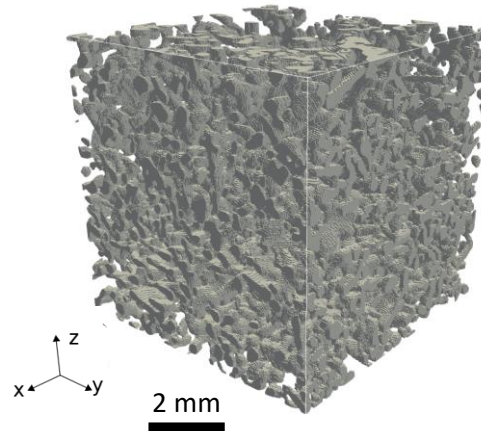


Experimental setup (Bernard et al., 2023)

Methodology: numerical setup



Binary segmentation



Homogeneous ice model 3D Norton law (*Suquet, 1983*)

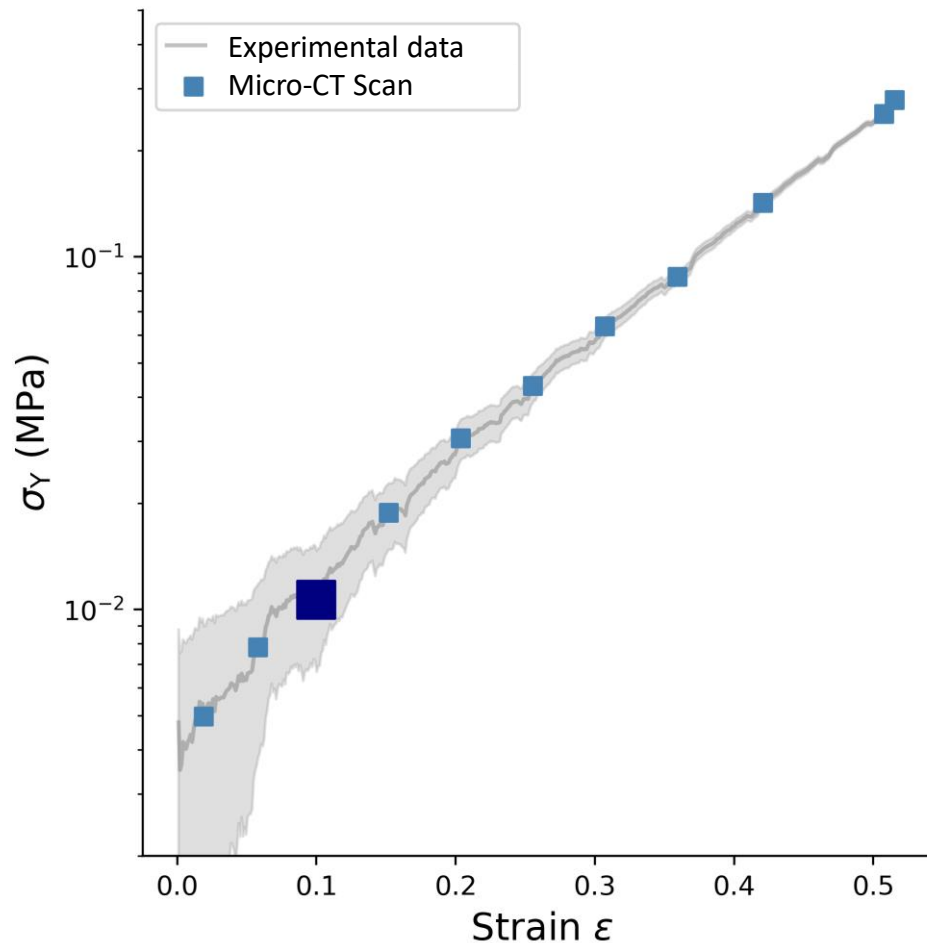
$$\epsilon = \epsilon_e + \epsilon_{vp}$$

$$\dot{\epsilon}_{vp} = \frac{3}{2} A \sigma_{eq}^{n-1} \boldsymbol{\sigma}'$$

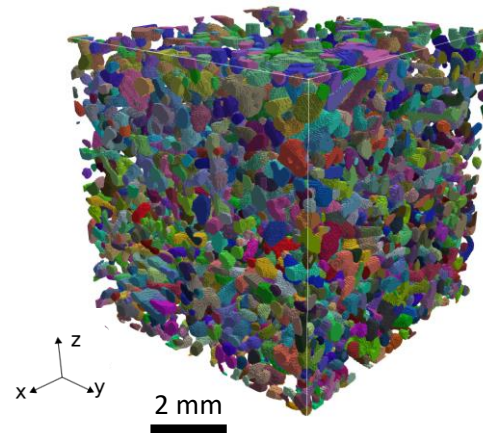
with σ_{eq} the equivalent stress, $\boldsymbol{\sigma}'$ the deviatoric stress, $A = 7.8 \cdot 10^{-8} \text{ MPa}^{-n} \text{ s}^{-1}$ and $n = 3$

From *Castelnau et al., 1998, Theile et al., 2011*

Methodology: numerical setup



Grain segmentation



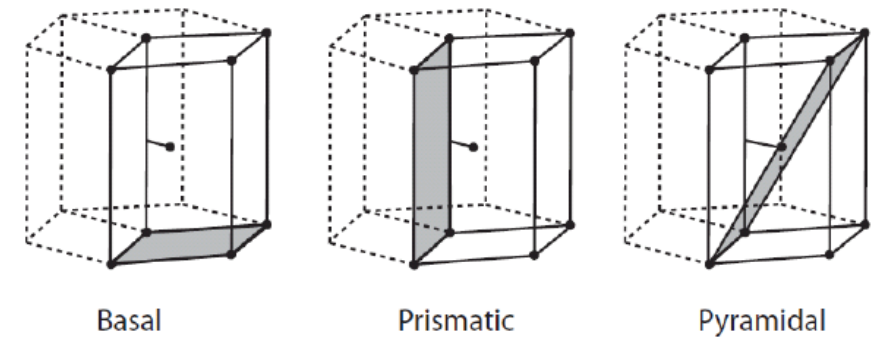
Sintered crystal model
Crystal plasticity

$$\epsilon_{vp} = \sum_{k=1}^{12} \gamma^{(k)} \mu^k$$

$$\mu^k = \frac{1}{2} (n^k \otimes_s b^k) \text{ the Schmid tensor}$$

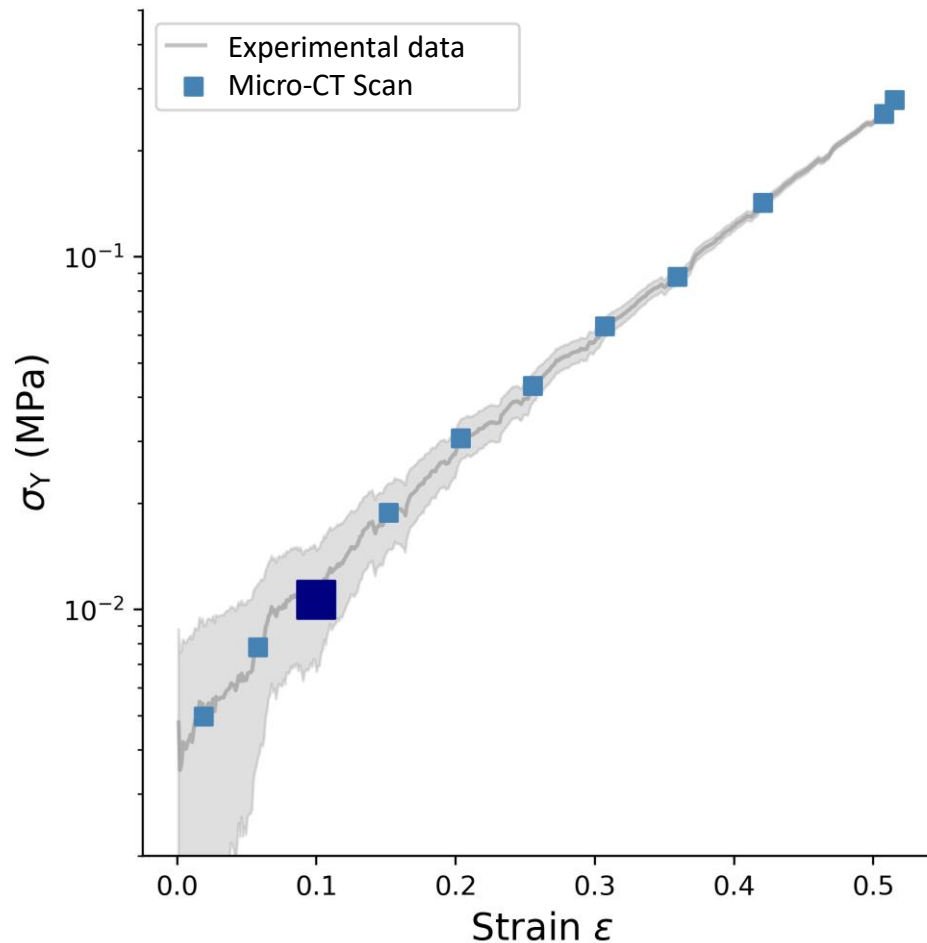
$$\dot{\gamma}^{(k)} = \dot{\gamma}_0^{(k)} \left(\frac{|\tau^{(k)}|}{\tau_0^k} \right)^{n^{(k)}} \text{sgn}(\tau^{(k)}) \text{ with } \tau^{(k)} = \sigma : \mu^k$$

with $\tau_0^{(k)}$ the reference resolved shear stress,
 $\dot{\gamma}_0^{(k)} = 1 \text{ s}^{-1}$ the reference shear rate

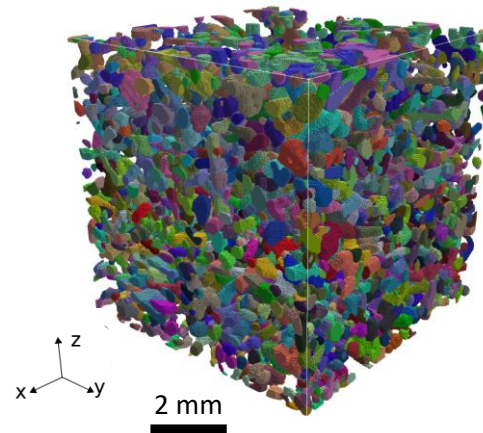


The three slip systems present in ice crystal (Poerschke, 2009)

Methodology: numerical setup



Grain segmentation



Sintered crystal model
Crystal plasticity

$$\epsilon_{vp} = \sum_{k=1}^{12} \gamma^{(k)} \mu^k$$

$$\mu^k = \frac{1}{2} (n^k \otimes_s b^k) \text{ the Schmid tensor}$$

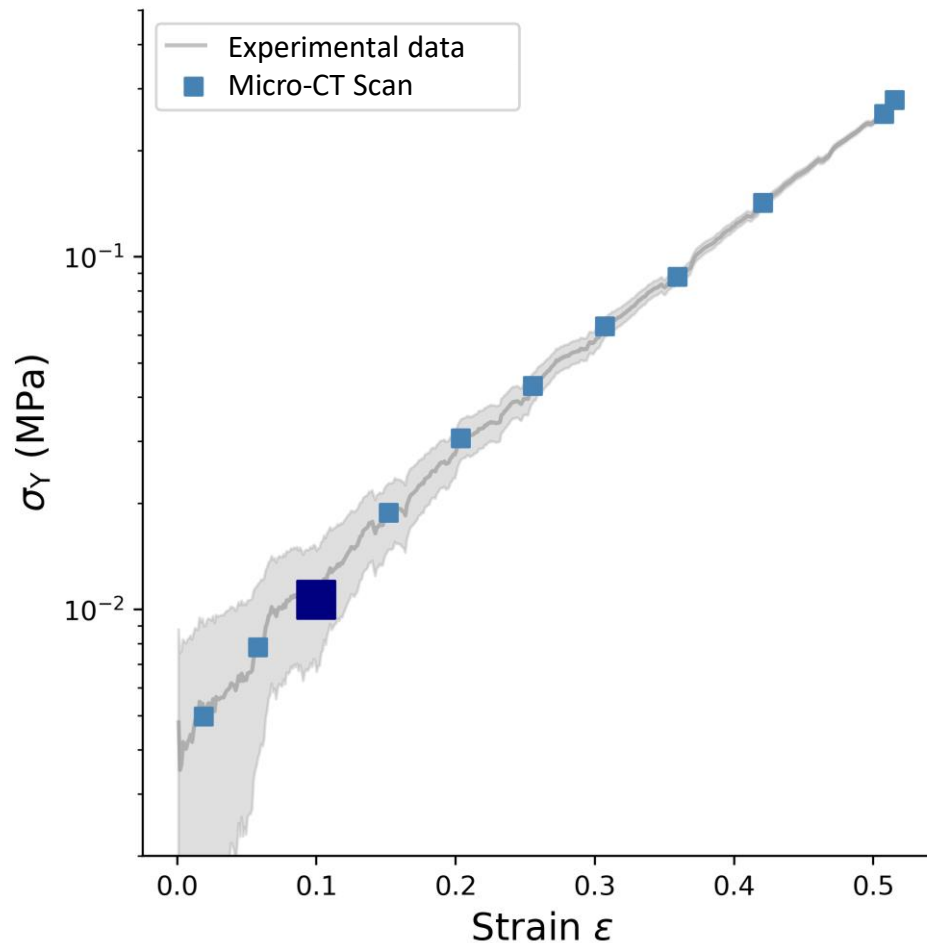
$$\dot{\gamma}^{(k)} = \dot{\gamma}_0^{(k)} \left(\frac{|\tau^{(k)}|}{\tau_0^k} \right)^{n^{(k)}} \text{sgn}(\tau^{(k)}) \text{ with } \tau^{(k)} = \sigma : \mu^k$$

with $\tau_0^{(k)}$ the reference resolved shear stress,
 $\dot{\gamma}_0^{(k)} = 1 \text{ s}^{-1}$ the reference shear rate

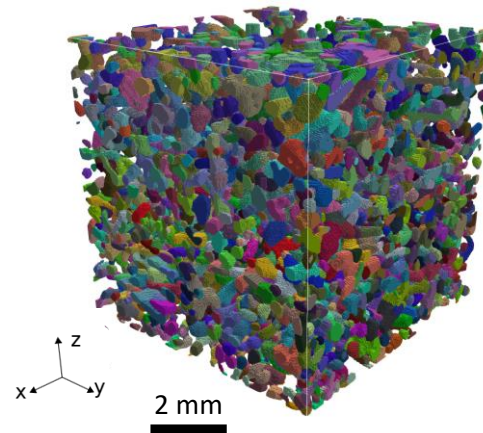
Family	Systems	$n^{(k)}$	$\tau_0^{(k)}$ (MPa)
Basal [0001]<11 $\bar{2}$ 0>	3	3	13
Prismatic [01 $\bar{1}$ 0]<2 $\bar{1}$ $\bar{1}$ 0>	3	3	260
Pyramidal [11 $\bar{2}$ 2]<11 $\bar{2}$ $\bar{3}$ >	6	3	260

*Monocrystalline ice parameters of viscoplastic model at -10°C
 adapted from Lebensohn et al., 2009 and Hondoh, 2000*

Methodology: numerical setup



Grain segmentation



Sintered crystal model
Crystal plasticity

$$\epsilon_{vp} = \sum_{k=1}^{12} \gamma^{(k)} \mu^k$$

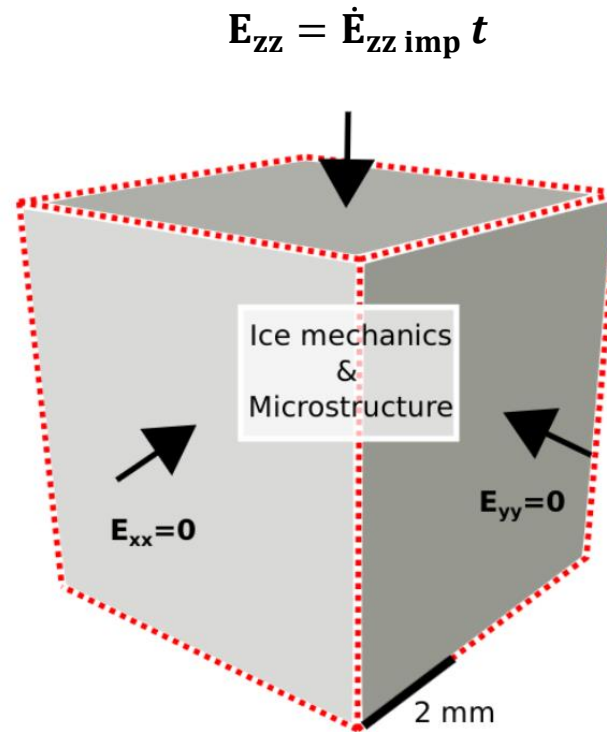
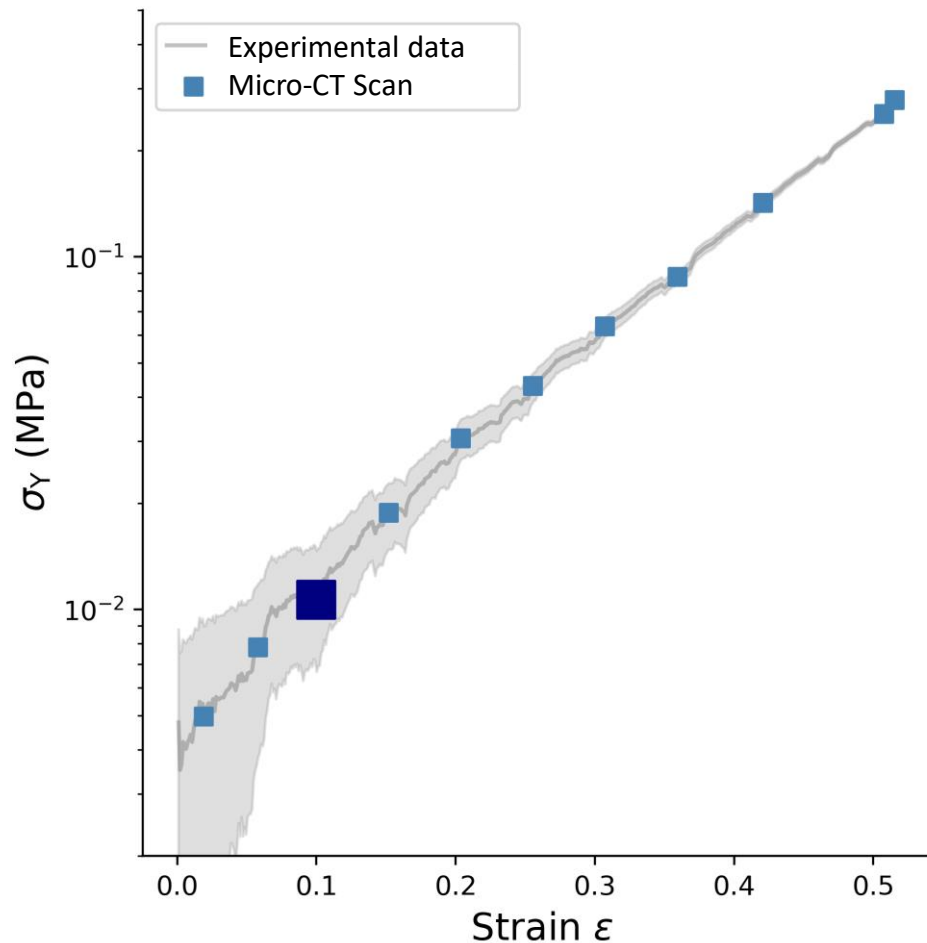
$$\mu^k = \frac{1}{2} (n^k \otimes_s b^k) \text{ the Schmid tensor}$$

$$\dot{\gamma}^{(k)} = \dot{\gamma}_0^{(k)} \left(\frac{|\tau^{(k)}|}{\tau_0^k} \right)^{n^{(k)}} \text{sgn}(\tau^{(k)}) \text{ with } \tau^{(k)} = \sigma : \mu^k$$

with $\tau_0^{(k)}$ the reference resolved shear stress,
 $\dot{\gamma}_0^{(k)} = 1 \text{ s}^{-1}$ the reference shear rate

→ Implemented with the
StandardElastoViscoPlasticity brick
 (Helfer et al., 2019)

Methodology: numerical setup



Hypothesis no lateral friction:

$$\Sigma_{xy} = \Sigma_{yz} = \Sigma_{xz} = 0$$

Use **AMITEX**
(Gélébart et al., 2020)

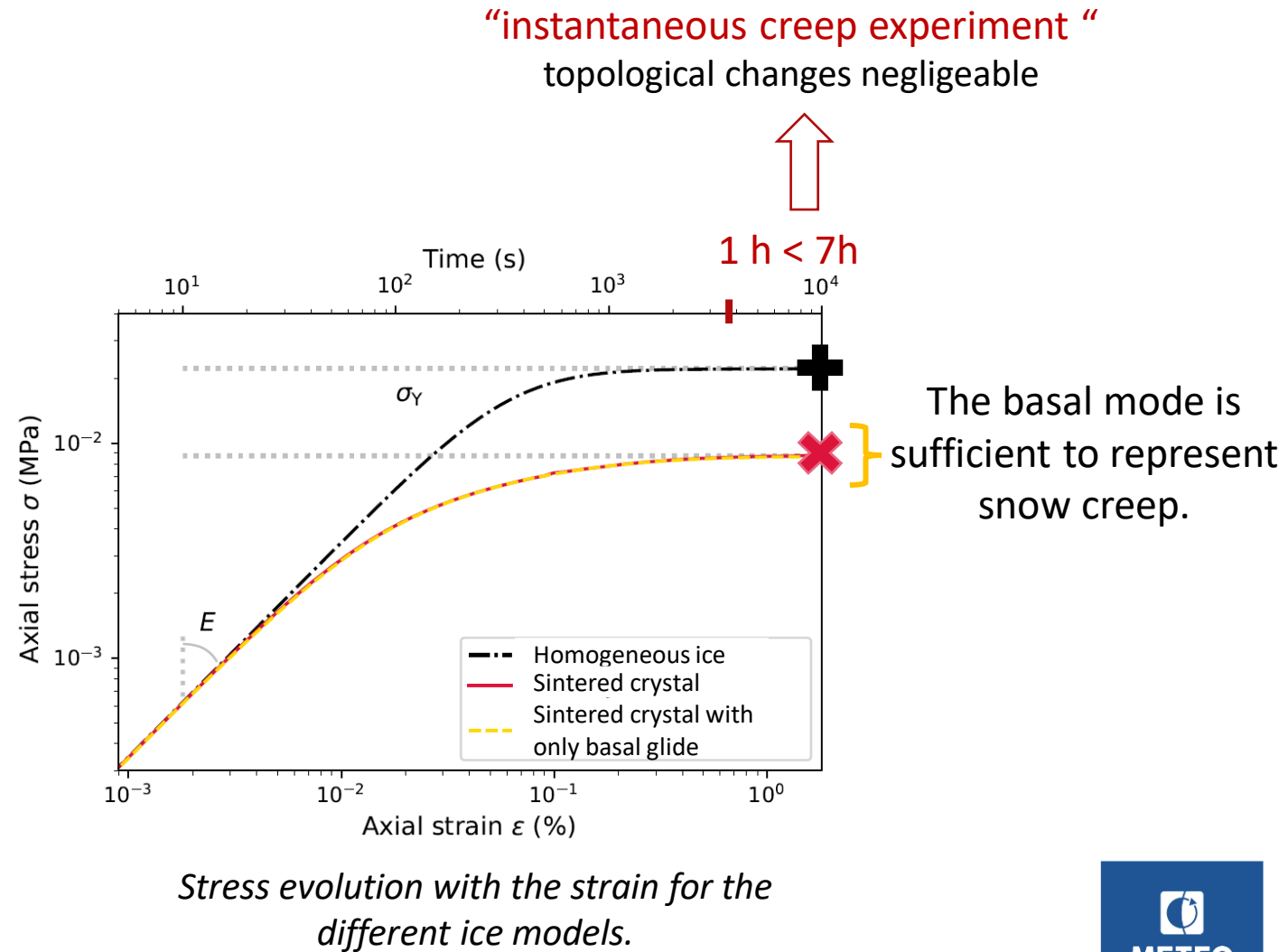
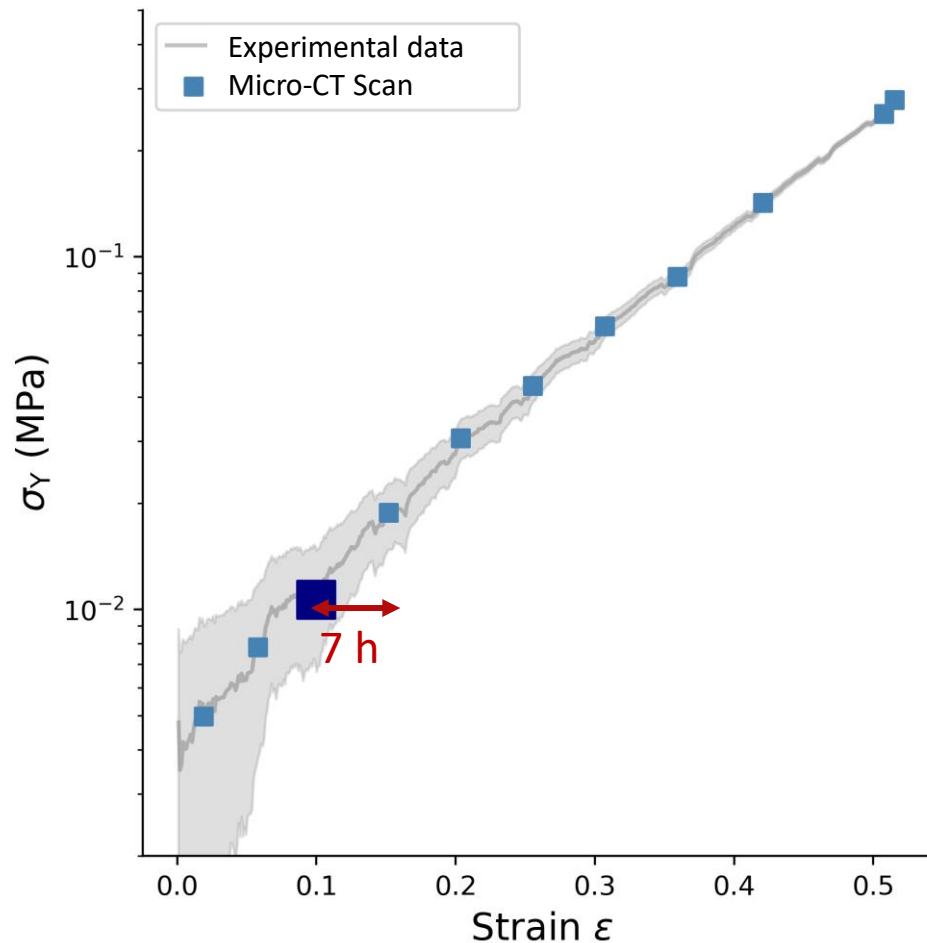
- Voxel images are the direct input of the simulations
- Benefits from the MPI parallelisation

Simulations on a Representative Elementary Volume (REV)

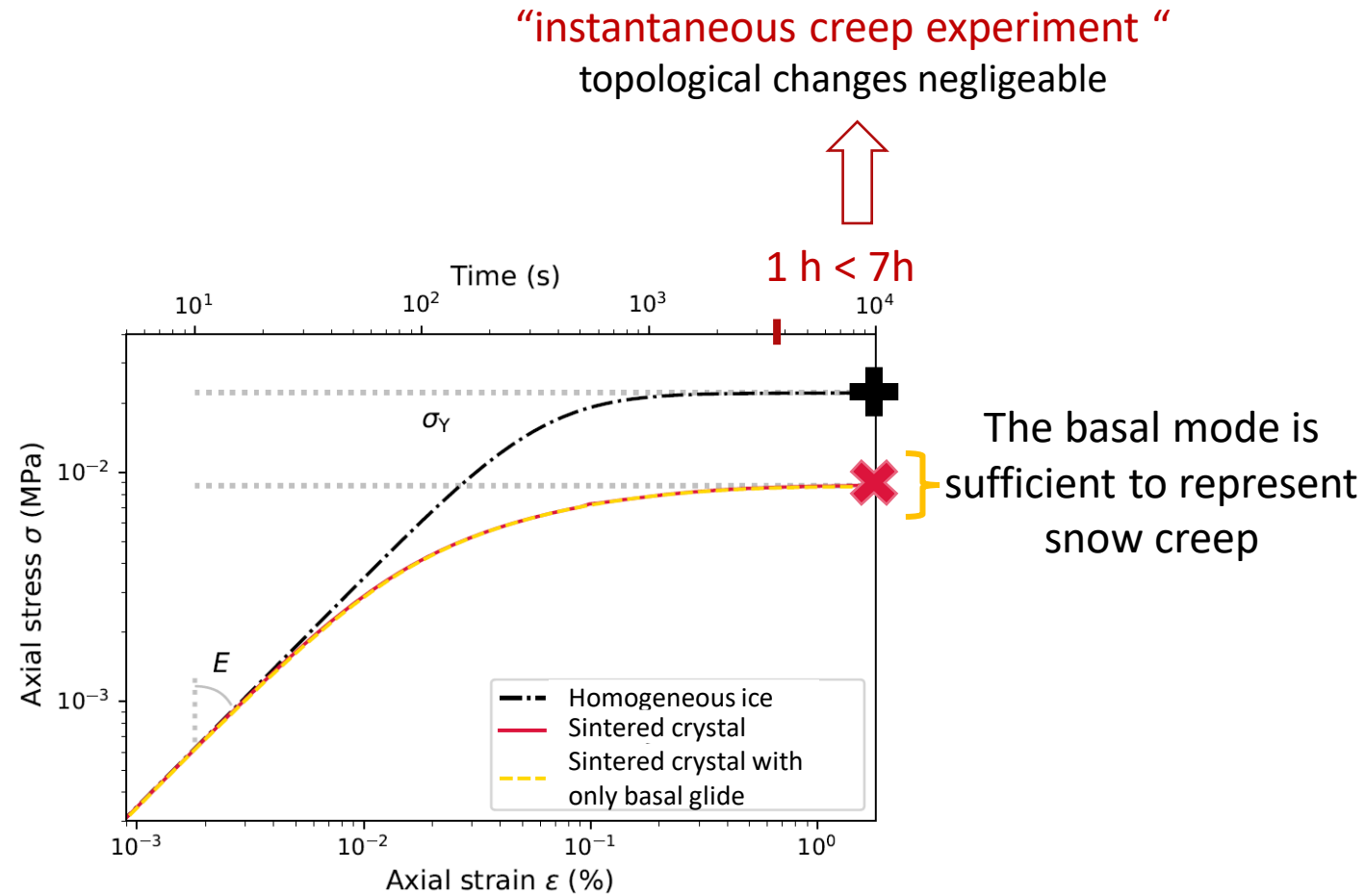
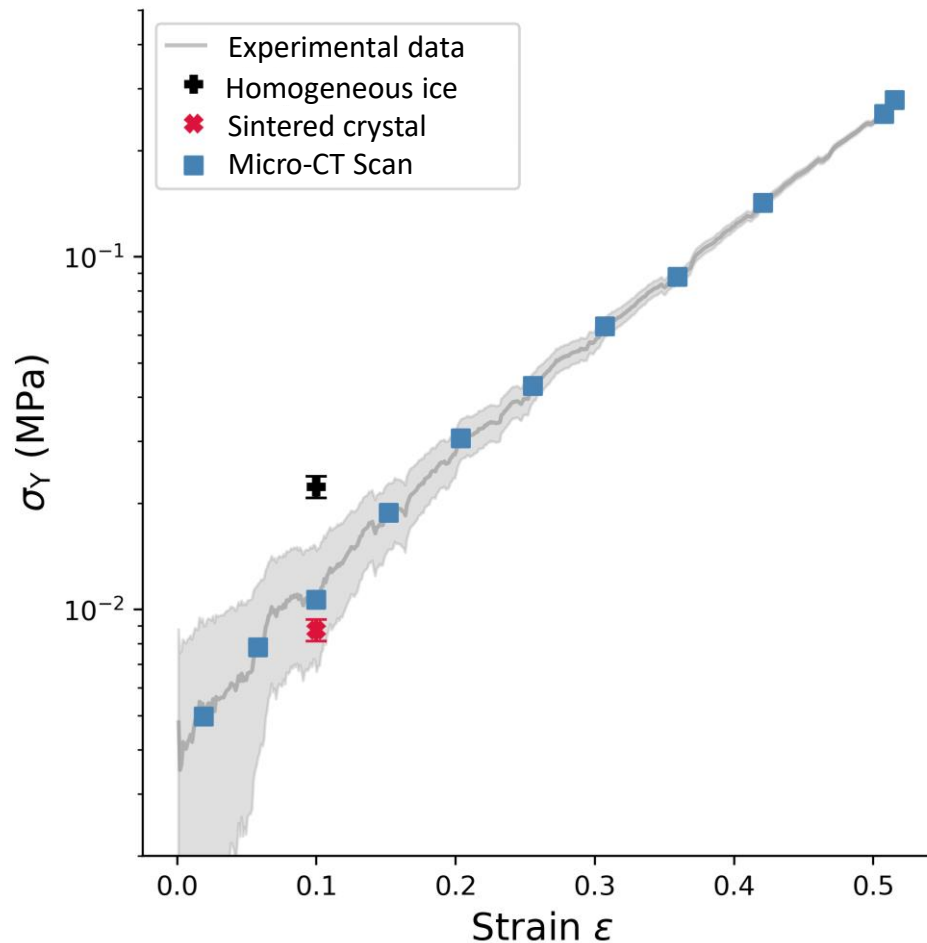
$$5.1 \times 5.1 \times 5.1 \text{ mm}^3$$

$$\text{as } L_{\text{macro}} \gg L_{\text{micro}}$$

Results: compression tests

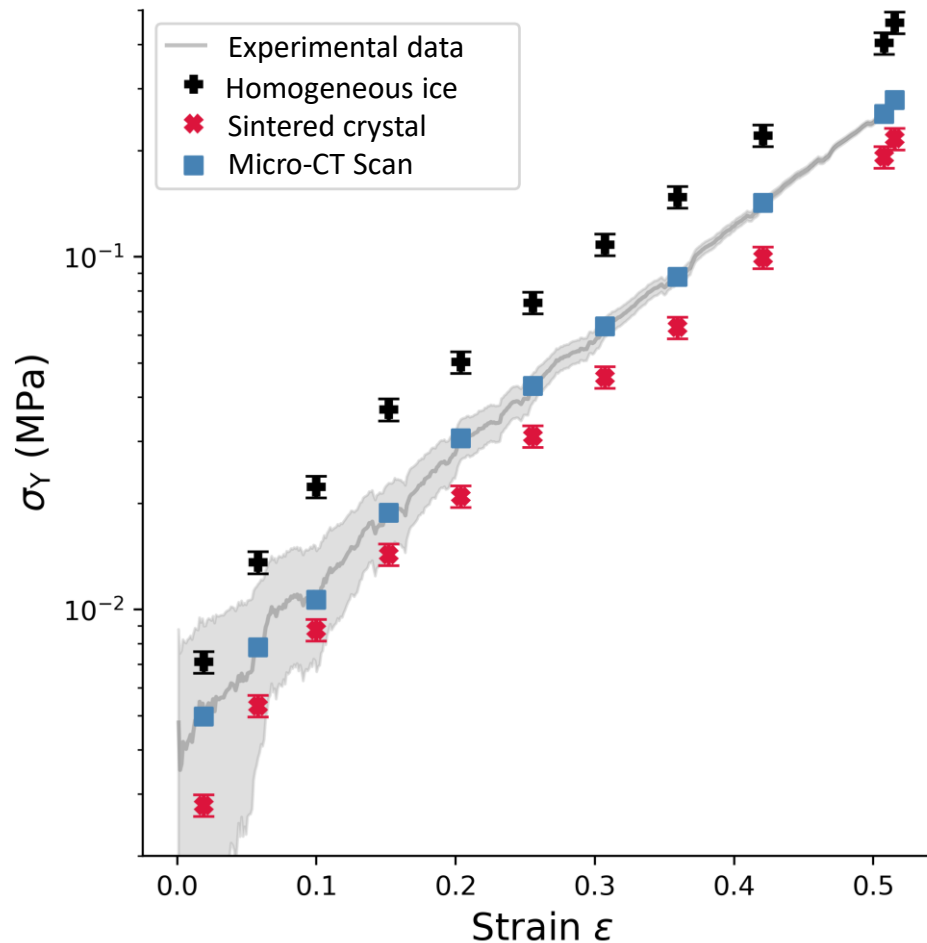


Results: experimental comparison



Stress evolution with the strain for the different ice models.

Results: experimental comparison



The same method is repeated for each scan ...

Study of the nonlinear viscosity:

$$B = \frac{\sigma^n}{\dot{\varepsilon}}$$

with $n=3$ by homogeneization (*Wautier et al., 2017*)

The same process is repeated for the **load-controlled test**

Results: experimental comparison

- Ice in snow should not be considered as a foam of ice,

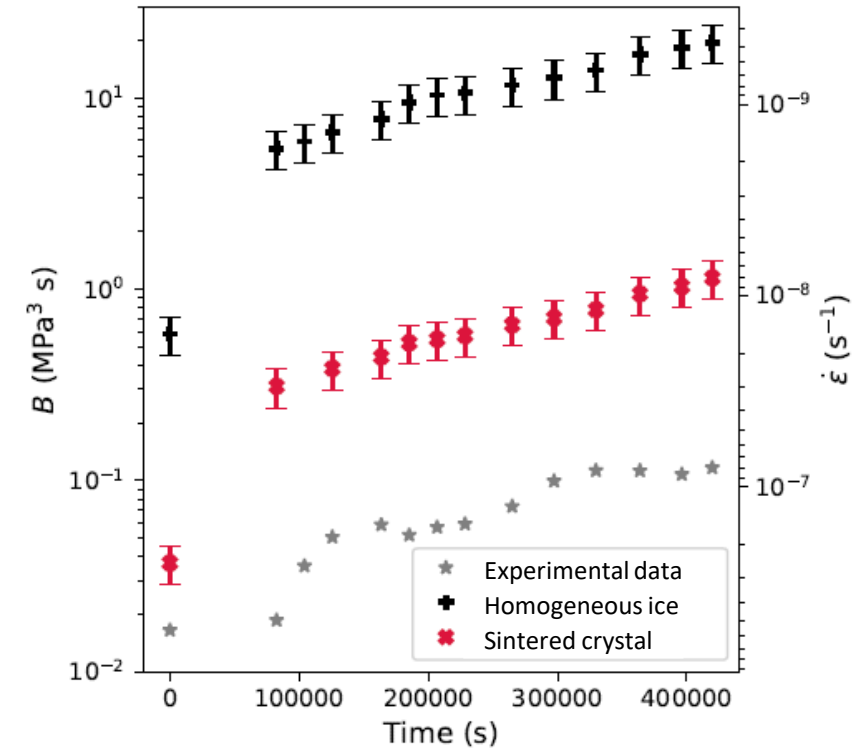
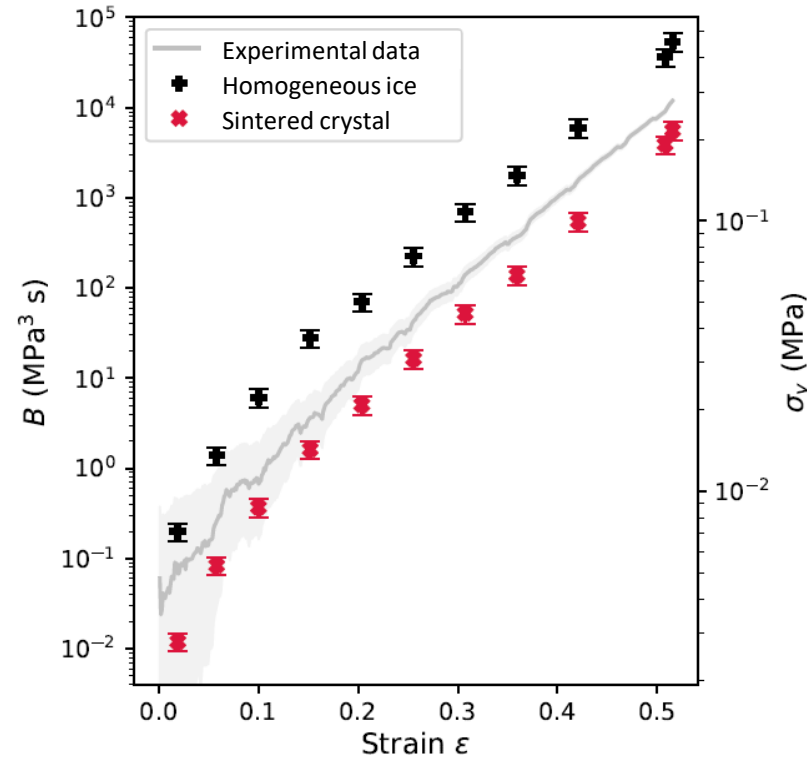


Homogeneous ice model



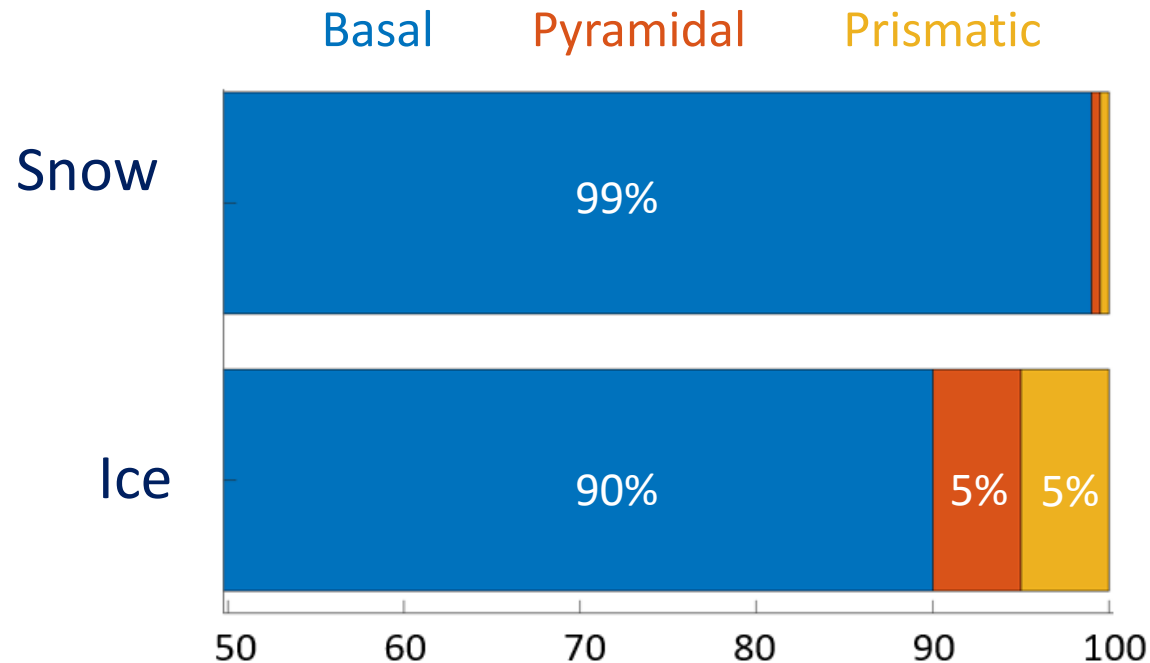
Sintered crystal model

- The gap between the two models decreases as density increases.



Results: microscopic aspects of snow creep

An accommodation of the basal slip different from ice!

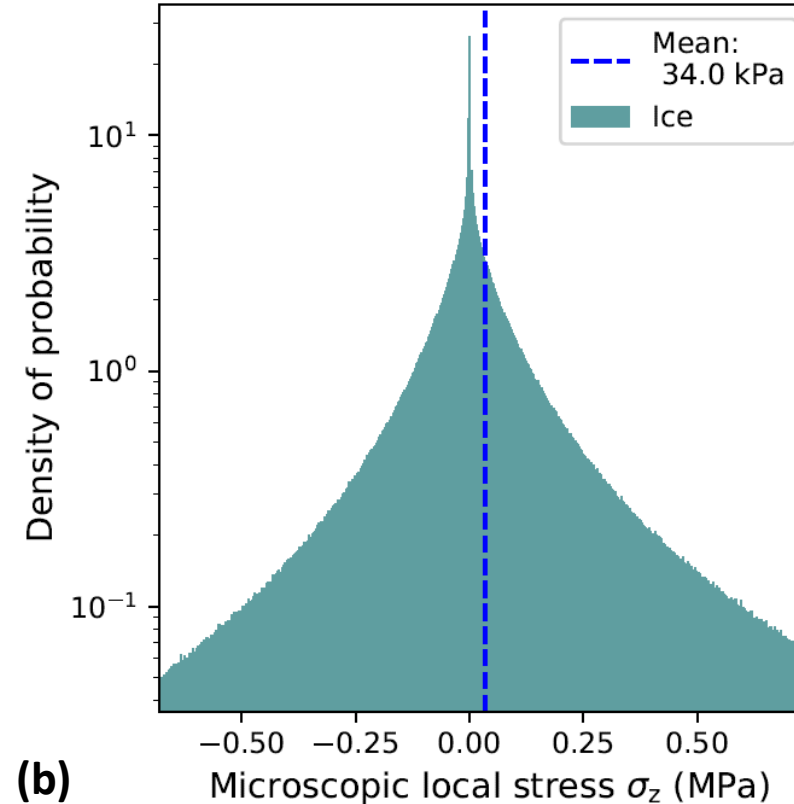
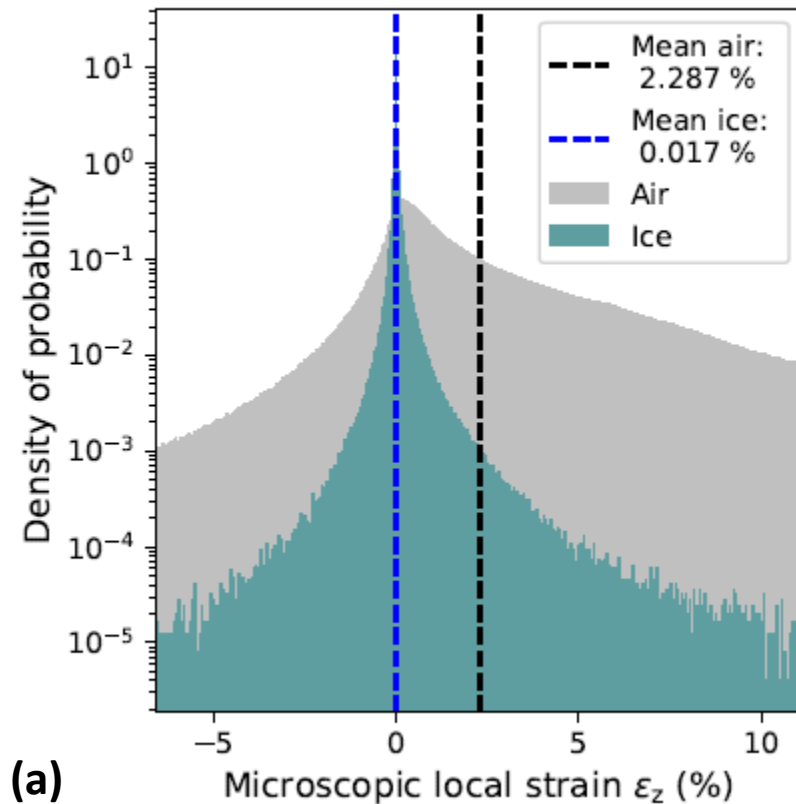


Contribution of the different glide systems on the microscopic equivalent slip (p_{eq})

- In snow : **accommodation** between crystals is permitted by the **pore space**



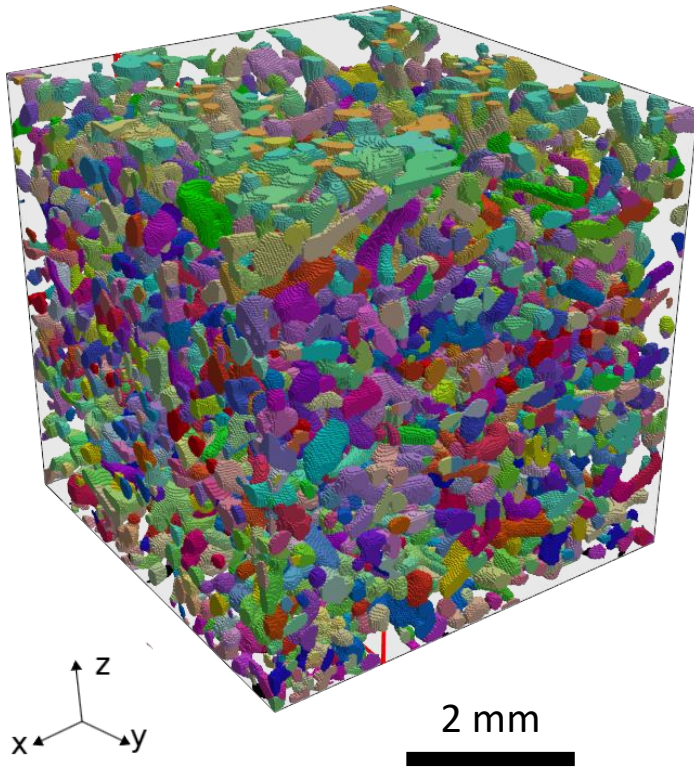
Results: microscopic aspects of snow creep



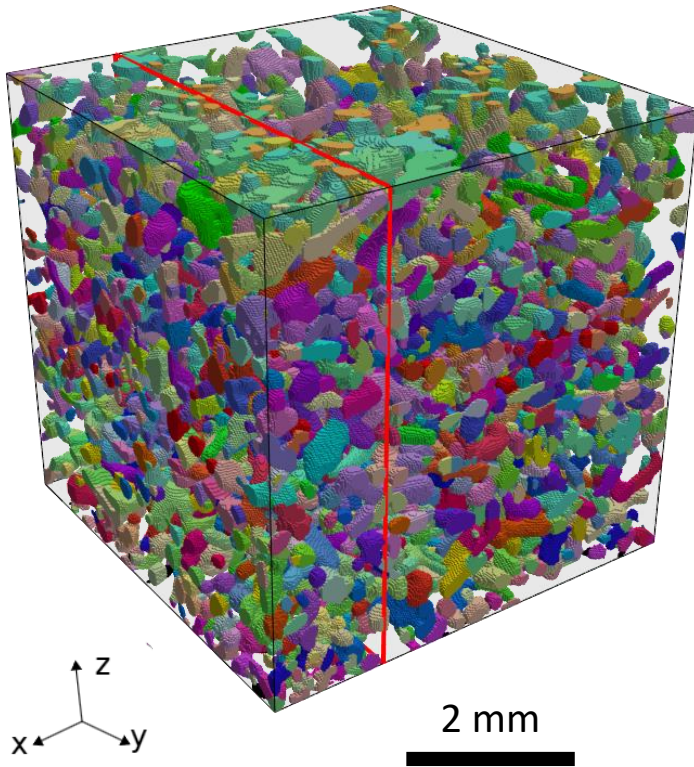
- Macroscopic deformation is mainly due to **air deformation** and accommodation of the ice matrix.
- **Hight stress concentration:** 5 % of the microstructure reaches a vertical stress value higher than 0.51 MPa (58 times the macroscopic loading).

Histogram of the microscopic: (a) local strain ϵ_z distribution, (b) vertical stress σ_z distribution.

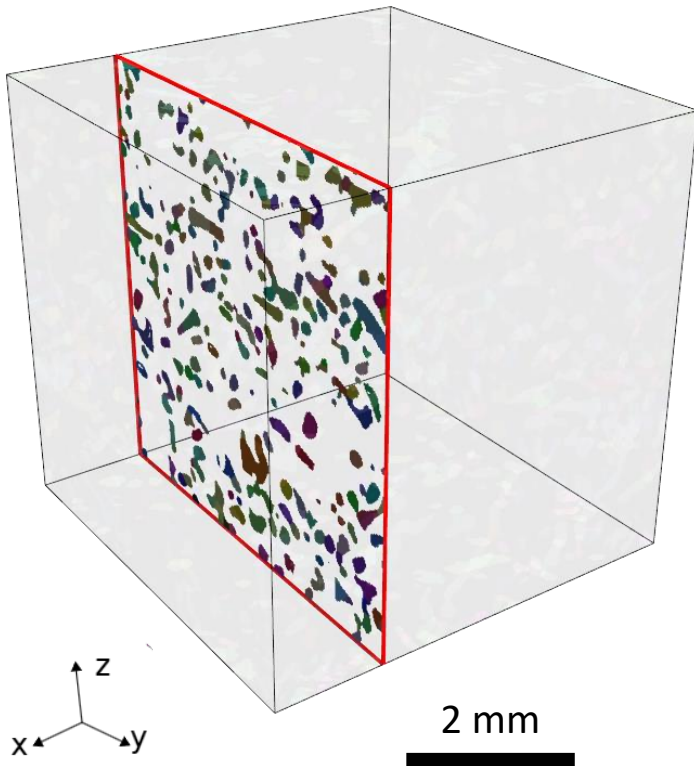
Results: microscopic aspects of snow creep



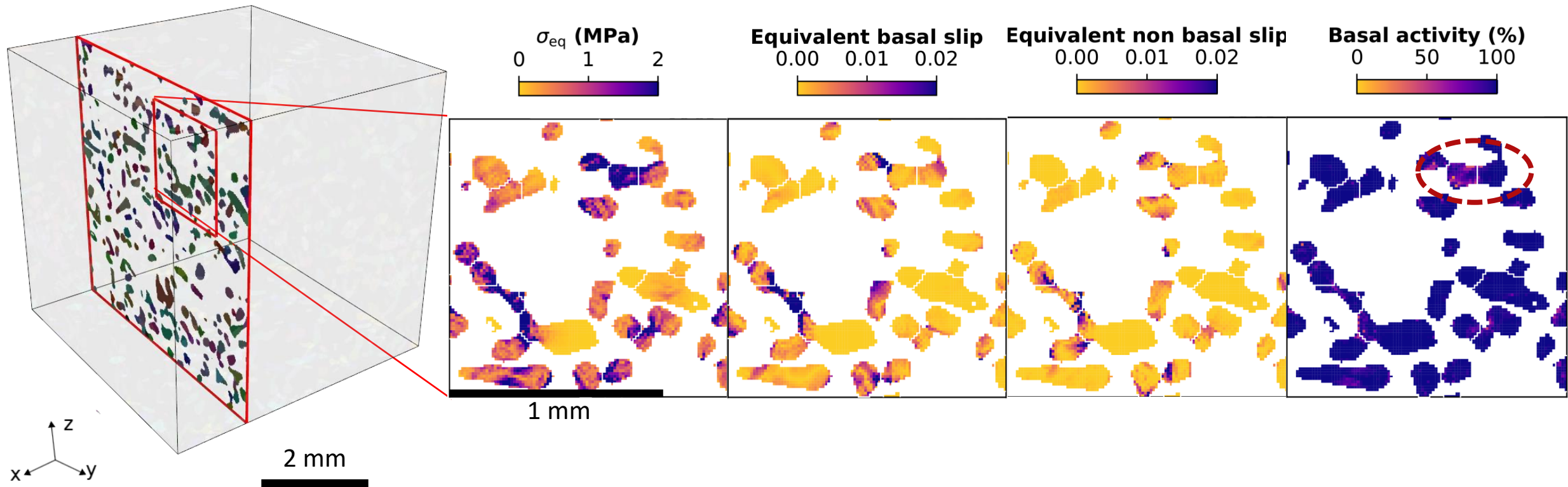
Results: microscopic aspects of snow creep



Results: microscopic aspects of snow creep



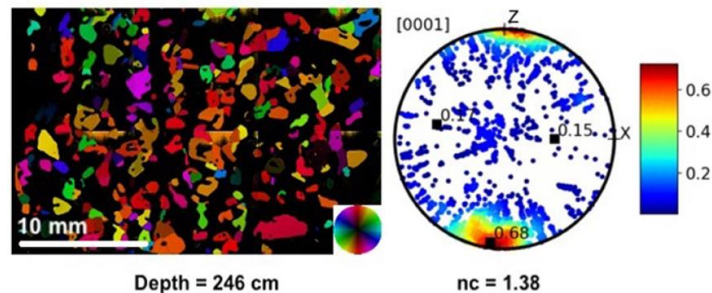
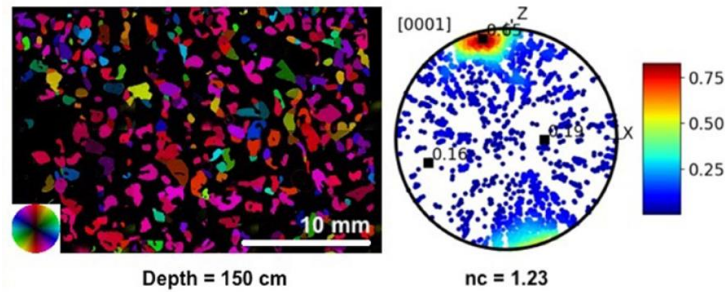
Results: microscopic aspects of snow creep



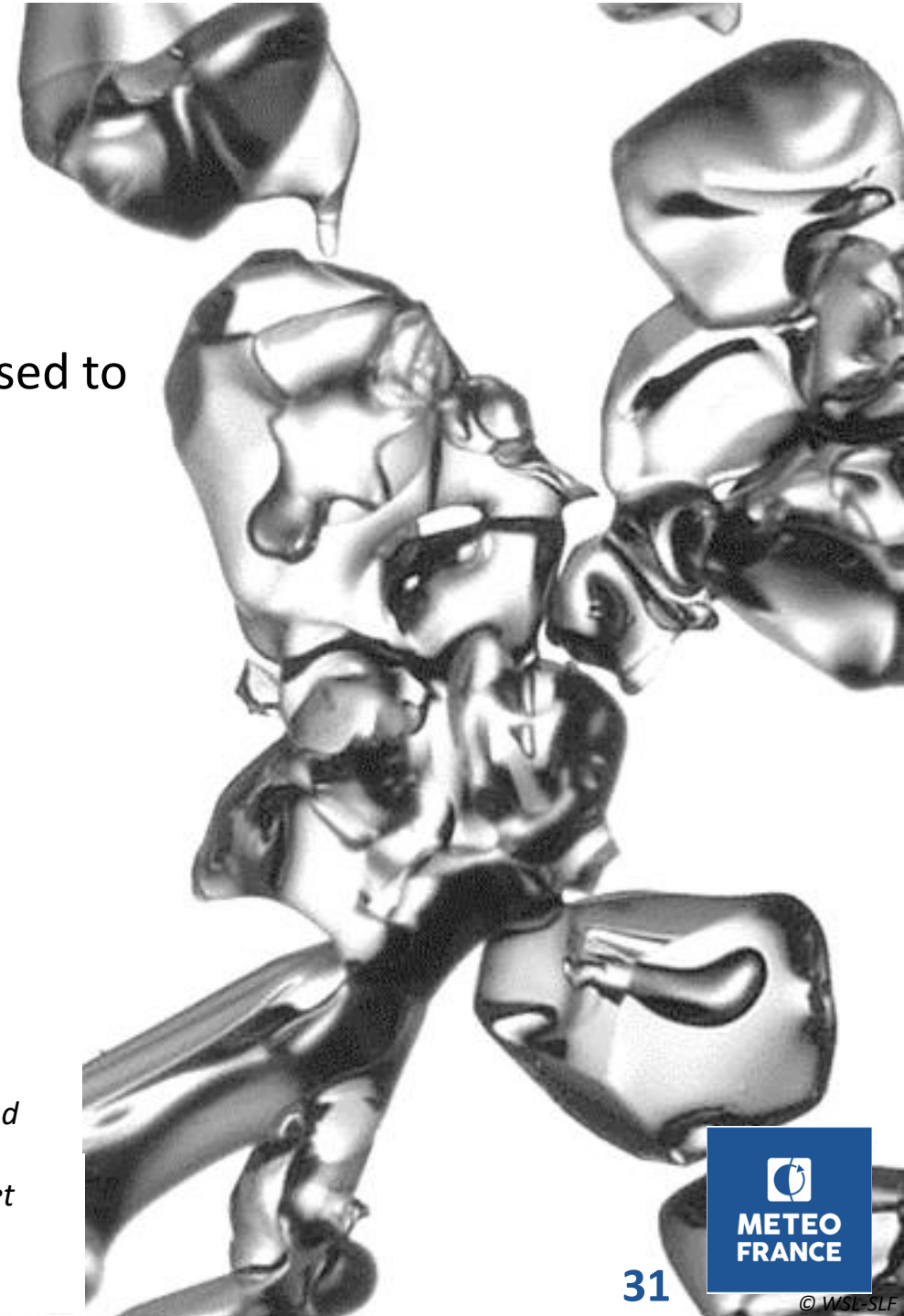
- Equivalent slip occurred preferentially at **crystal bond**, where stress is concentrated

Conclusion and outlooks

- First time that a **single-crystal plasticity model** has been used to study the mechanical behaviour of snow.
- Snow cannot be considered as a foam of ice, behaviour of **single-crystals** need to be considered.



Microstructure and C-axis pole figure from samples extracted at 150 (A) and 246 (B) cm depth along the EastGRIP snow pit (adapted from Montagnat et al., 2020)



Conclusion and outlooks

- First time that a **single-crystal plasticity model** has been used to study the mechanical behaviour of snow.
- Snow cannot be considered as a foam of ice, behaviour of **single-crystals** need to be considered.
- Micro-scale mechanisms not yet understood, particularly at **grain boundaries**. Hypothesis:
 - Superplasticity (Alley, 1987, Raj & Ashby, 1971)
 - Ductile failure (Kirchner et al. 2001)

→ New behaviour to model and further experiments planned



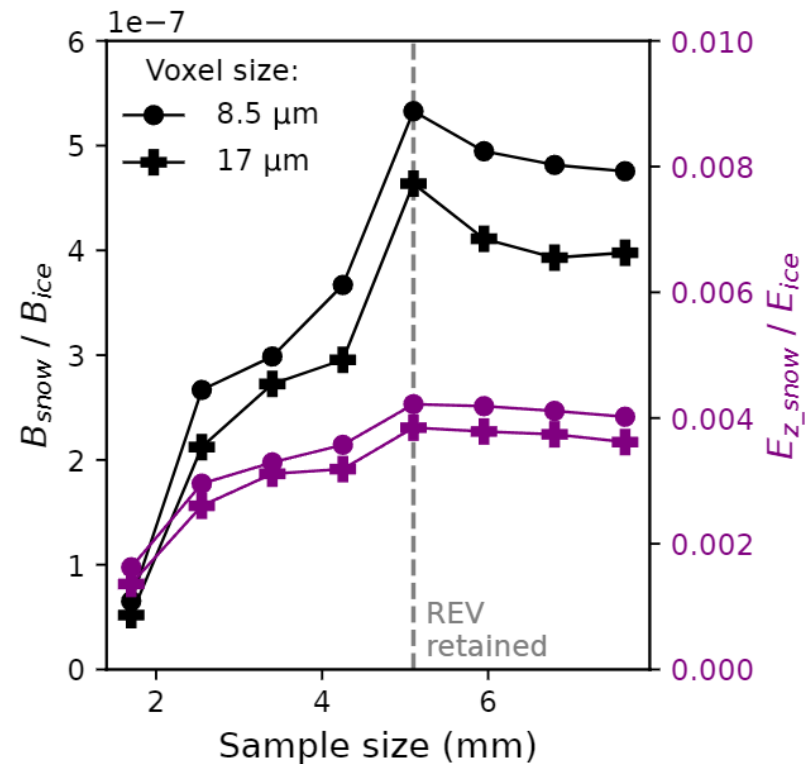
References

- Alley, R. B. (1987). Firn densification by grain-boundary sliding: a first model. *Journal de Physique*, 48 , 249–256.
- Bernard, A., Hagenmuller, P., Montagnat, M., & Chambon, G. (2022, 12). Disentangling creep and isothermal metamorphism during snow settlement with X-ray tomography.
- Bernard, A. (2023). Etude multi échelle de la transition ductile-fragile dans la neige (Doctoral dissertation, Université Grenoble Alpes).
- Gélébart, L., Derouillat, J., Doucet, N., Ouaki, F., Marano, A., & Duverge, J. (2020). AMITEX FFTP.
- Thomas Helfer, Olivier Fandeur, David Haboussa, Dominique Deloison, Olivier Jamond, et al.. New functionalities of the 3.0 version of TFEL, MFront and MTest. CSMA 2017 - 13e Colloque National en Calcul des Structures, IMSIA; LMS; Onera; DMEP (CEA), May 2017, Giens, France.
- Kirchner, H. O., Michot, G., Narita, H., & Suzuki, T. (2001). Snow as a foam of ice: Plasticity, fracture and the brittle-to-ductile transition. *Philosophical Magazine A*, 81 (9), 2161–2181.
- Lebensohn, R. A., Montagnat, M., Mansuy, P., Duval, P., Meyssonier, J., & Philip, A. (2009). Modeling viscoplastic behavior and heterogeneous intracrystalline deformation of columnar ice polycrystals. *Acta Materialia*, 57 (5), 1405–1415.
- Montagnat, M., Castelnau, O., Bons, P. D., Faria, S. H., Gagliardini, O., Gillet-Chaulet, F., . . . Suquet, P. (2014).
- Peinke, I., Hagenmuller, P., Ando, E., Chambon, G., Flin, F., & Roule, J. (2020,3). Experimental Study of Cone Penetration in Snow Using X-Ray To-mography. *Frontiers in Earth Science*, 8 , 63.
- Raj, R., & Ashby, M. F. (1971). On grain boundary sliding and diffusional creep. 2 (4), 1113–1127.
- Suquet, P. M. (1993). Overall potentials and extremal surfaces of power law or ideally plastic composites. *Journal of the Mechanics and Physics of Solids*, 41 (6), 981–1002.
- Theile, T., Lowe, H., Theile, T., & Schneebeli, M. (2011). Simulating creep of snow based on microstructure and the anisotropic deformation of ice. *Acta Materialia*, 59 (18), 7104–7113.
- Wautier, A., Geindreau, C., & Flin, F. (2017, 6). Numerical homogenization of the viscoplastic behavior of snow based on X-ray tomography images. *The Cryosphere*, 11 (3), 1465–1485.

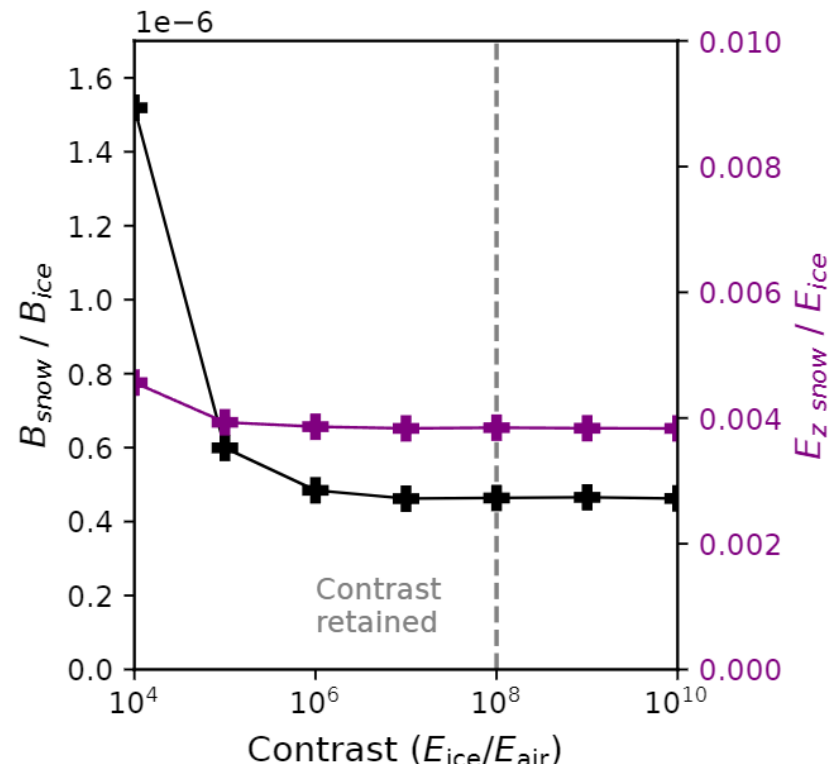
Appendix

Sensitivity analysis

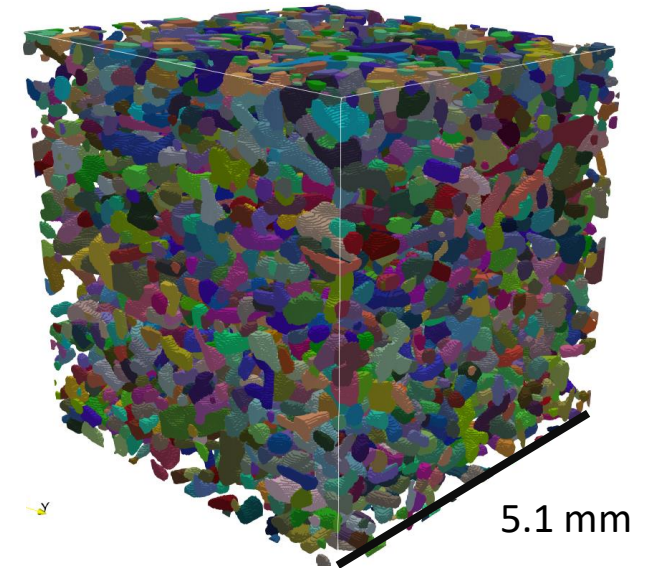
Representative Elementary Volume
and mechanical contrast



(a)



(b)



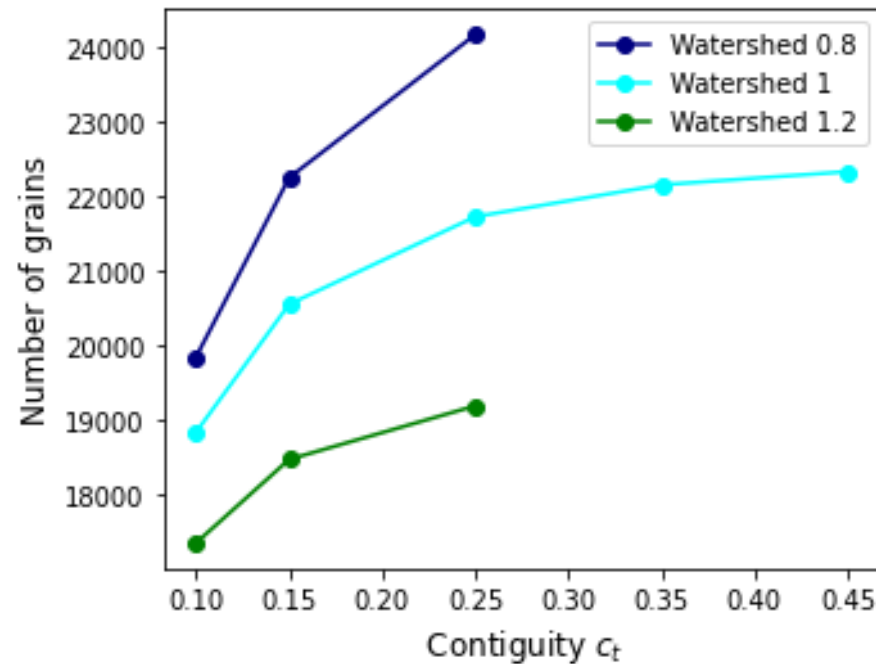
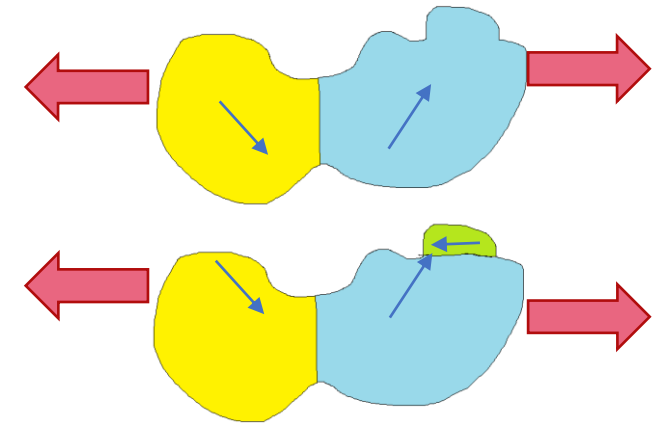
Sample studied.
Voxel size: 17 μm
 $\rho = 255 \text{ kg m}^{-3}$, $r_{eq} = 121 \mu\text{m}$,

Convergence analysis of the nonlinear viscosity and Young's modulus with respect to: (a) the sample length and (b) the mechanical contrast.

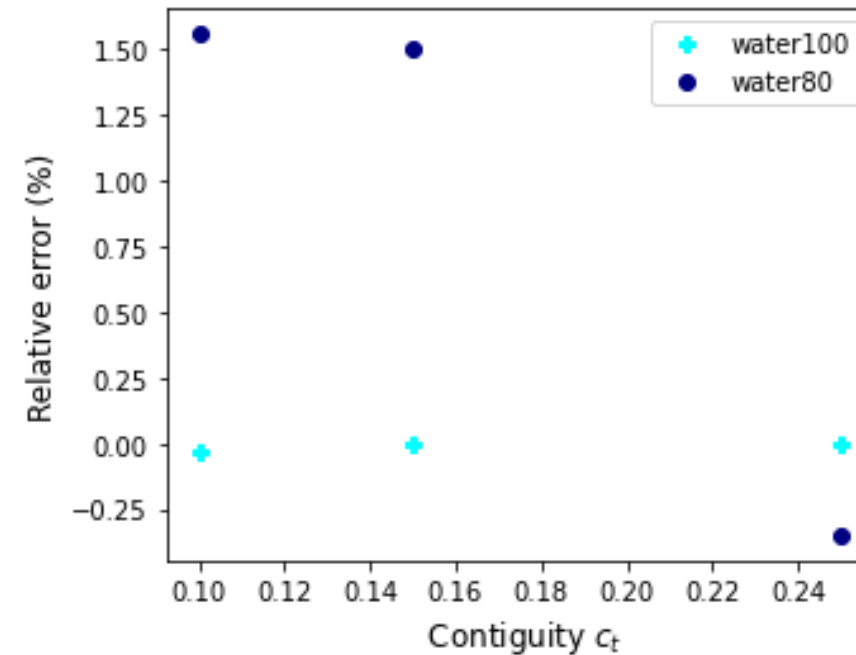
Sensitivity analysis

Grain segmentation

Low effect compared to uncertainty (REV, temperature, experimental measurement)

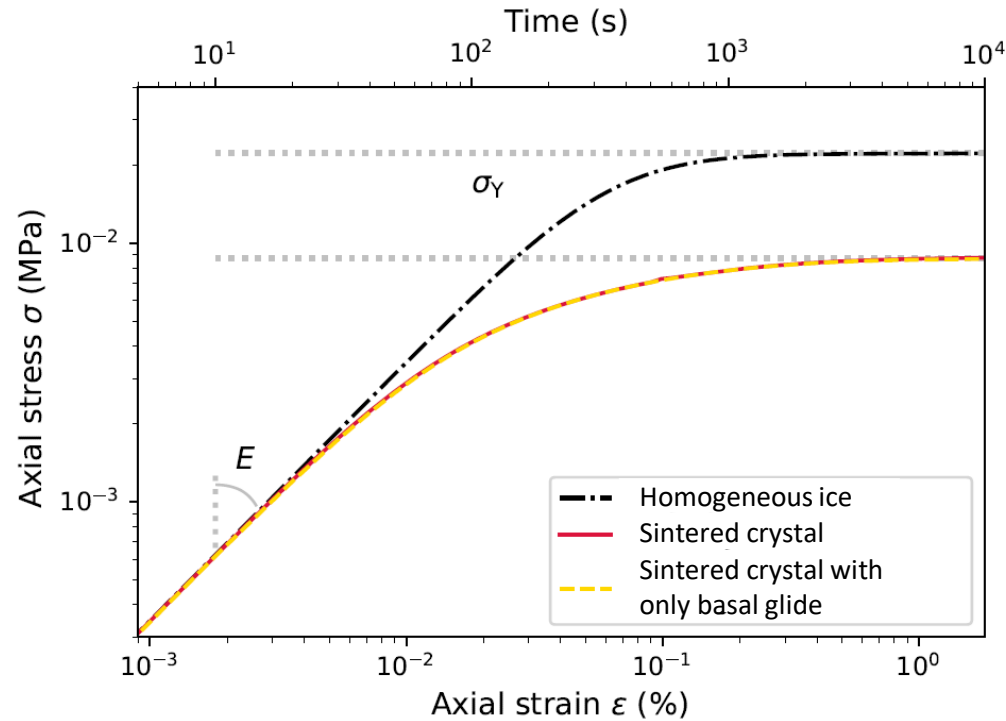


Number of geometrical grains as a function of c_t for different values of \tilde{k}_t .

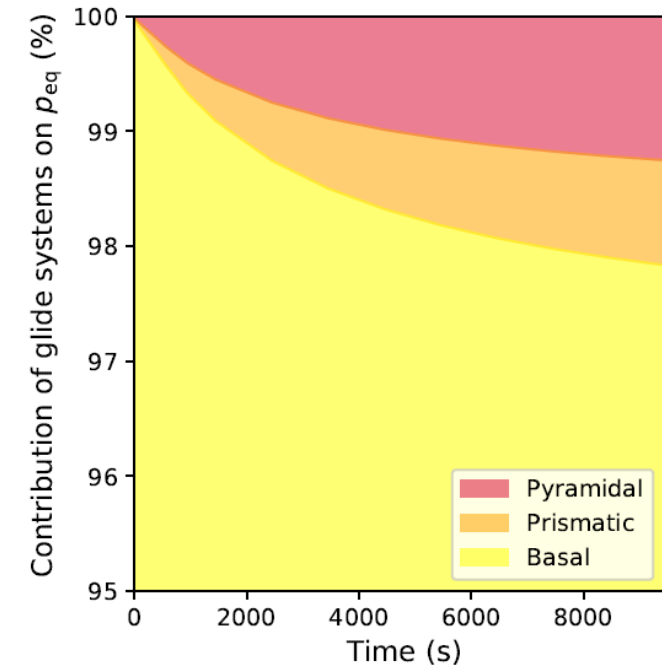


Relative error in the calculation of the snow B as a function of c_t for different values of \tilde{k}_t (reference $c_t = 0.15$; $\tilde{k}_t = 1$)

Influence of non-basal slip systems:



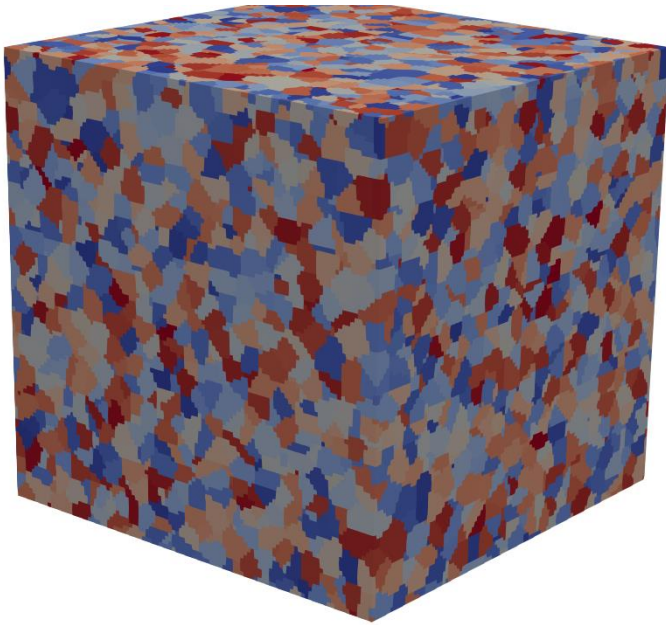
Evolution of yield stress with the strain for the different constitutive equations of ice.



Temporal evolution of the contribution of the different glide systems on the microscopic equivalent slip (p_{eq})

Preliminary study:

Modelling of the viscoplastic behaviour of ice



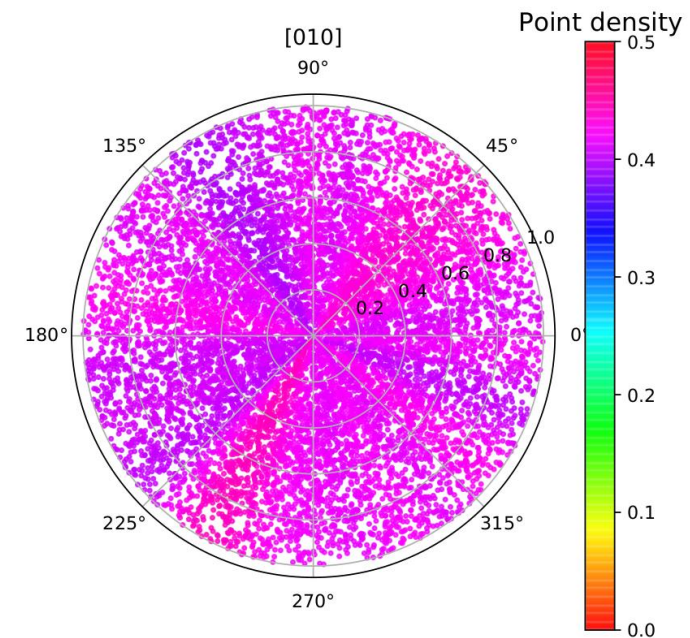
Voronoi, 9261 grains, 106^3 voxels

Boundary conditions:

Constant strain rate compression test with stress-free boundary condition

Implementation of the two material laws:

- polycrystalline
- monocrystalline: unknown grain orientation, random draw c-axis



Pole figure, plan (X,Z)

Elasto-viscoplasticity: preliminary study

Modelling of the viscoplastic behaviour of ice

Macroscopic laws identified:

- Polycrystalline model:

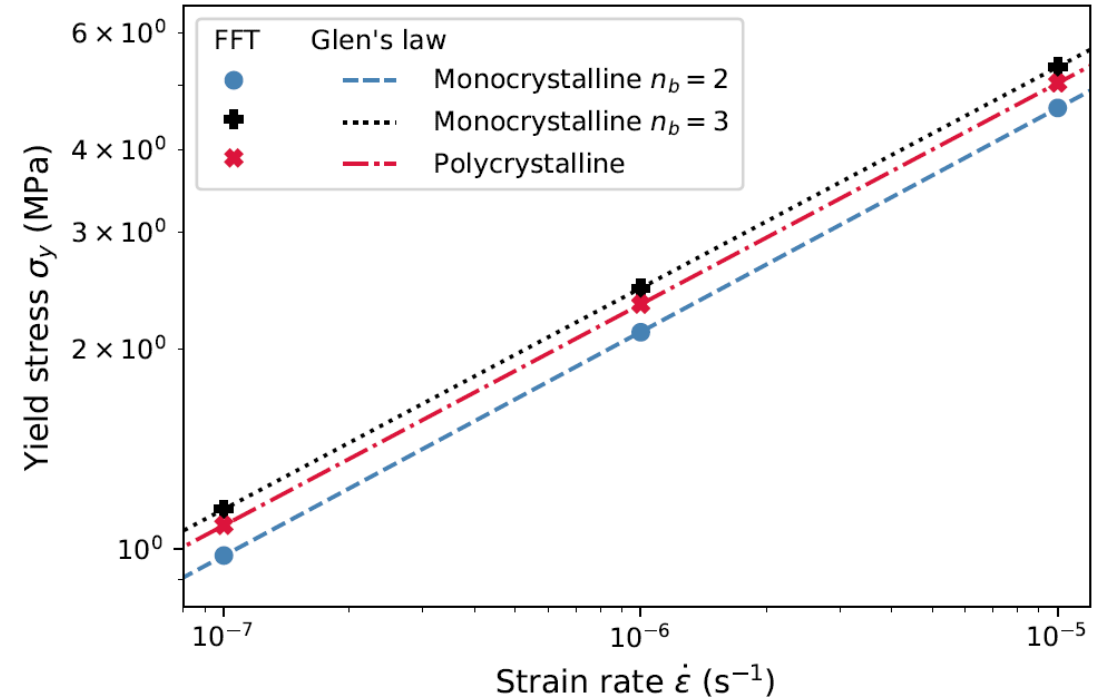
$$\dot{\epsilon} = 7.8 \times 10^{-8} \sigma_Y^3$$

- Monocrystalline model ($n_{basal} = 3$):

$$\dot{\epsilon} = 6.59 \times 10^{-8} \sigma_Y^3$$

- Macroscopic laws identified ($n_{basal} = 2$):

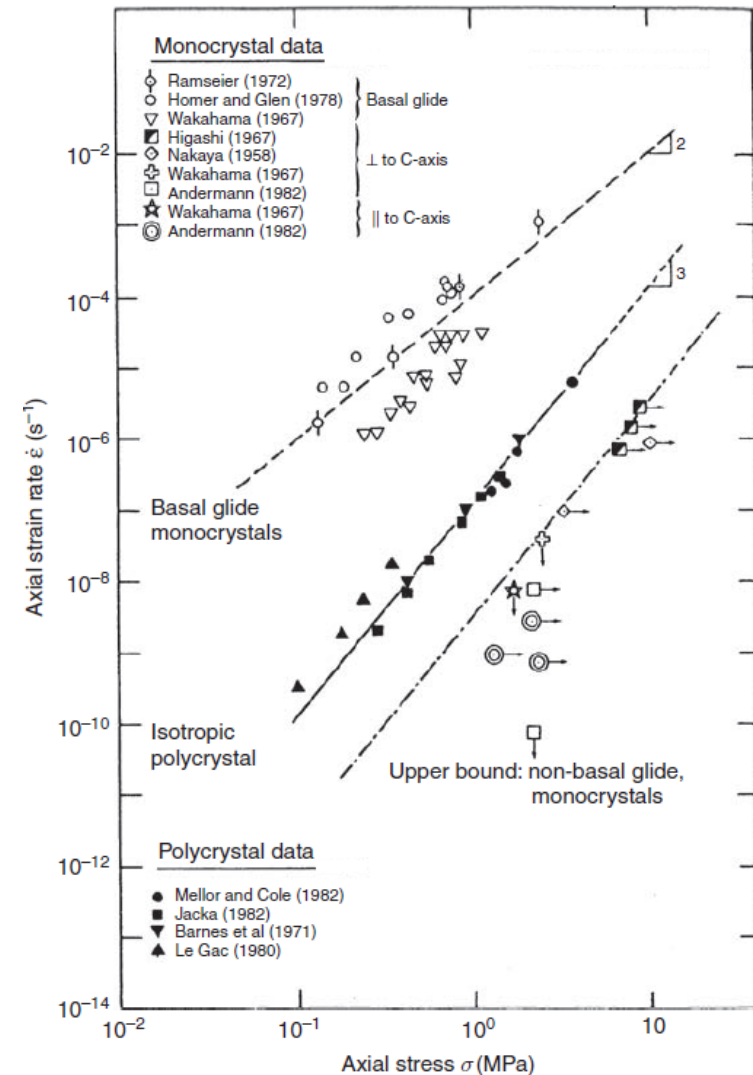
$$\dot{\epsilon} = 1.12 \times 10^{-8} \sigma_Y^{2.96}$$



- Simplified geometry
- Incertainties on the prefactor A of $\pm 25\%$
 - Negligible compared to error committed on snow

Limits and outlooks

- Basal slip system is main deformation mechanism
- Experiments show that basal slip system has an exponent **2** (3 for all systems in our study)
 - ! ➤ need to **calibrate a new crystal plasticity** model on polycrystalline ice
- **Homogenization of an elasto-viscoplastic law** for a wide range of snow microstructures, to develop improved formulations of snow settlement in detailed snowpack simulation tools.



Stress–strain rate relationship for steady-state basal and non-basal slip in single crystals at -10°C . (Schulson and Duval, 2009)